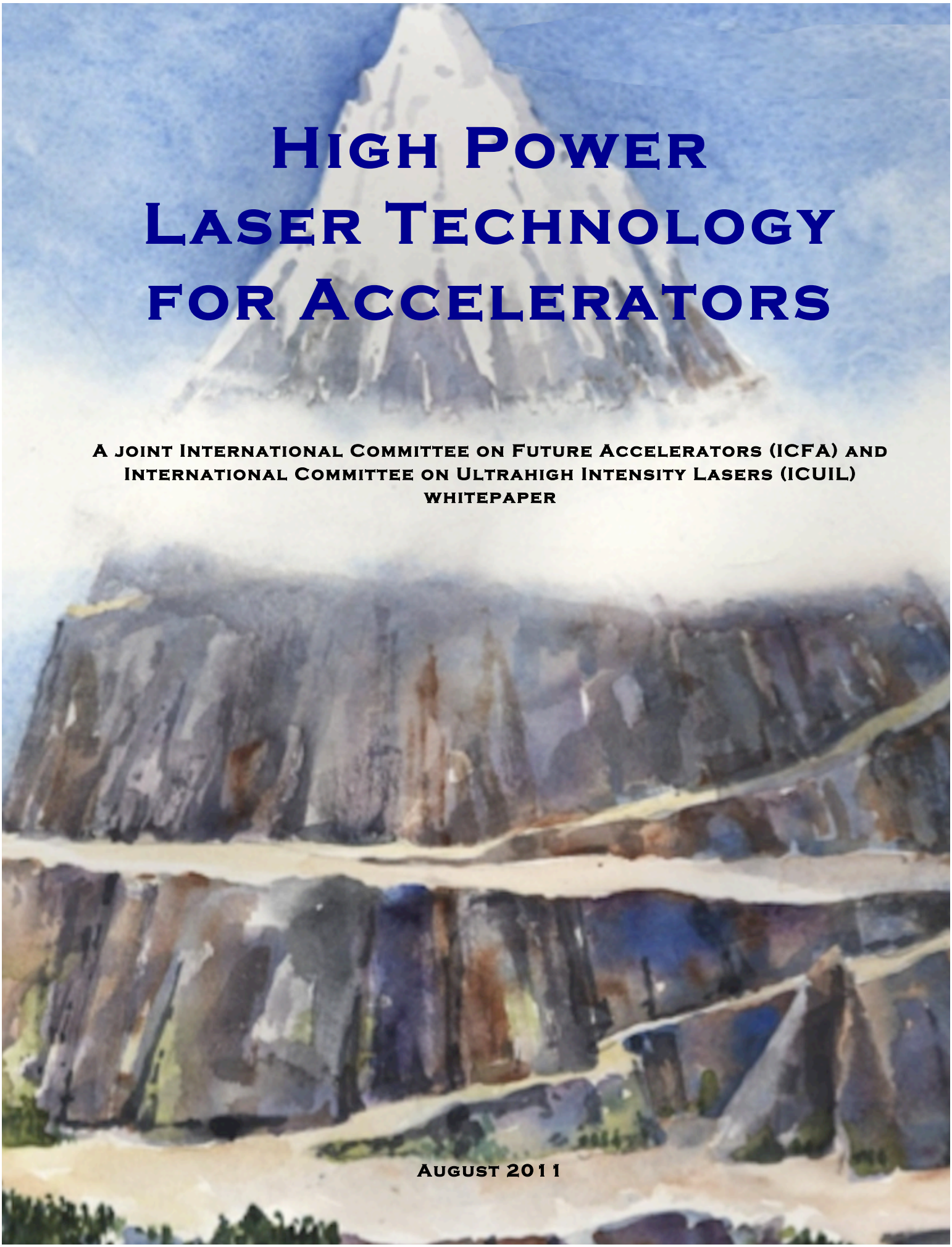

High Power Laser Technology for Accelerators

A joint International Committee on Future Accelerators (ICFA) and International Committee on Ultrahigh Intensity Lasers (ICUIL) whitepaper

August 2011

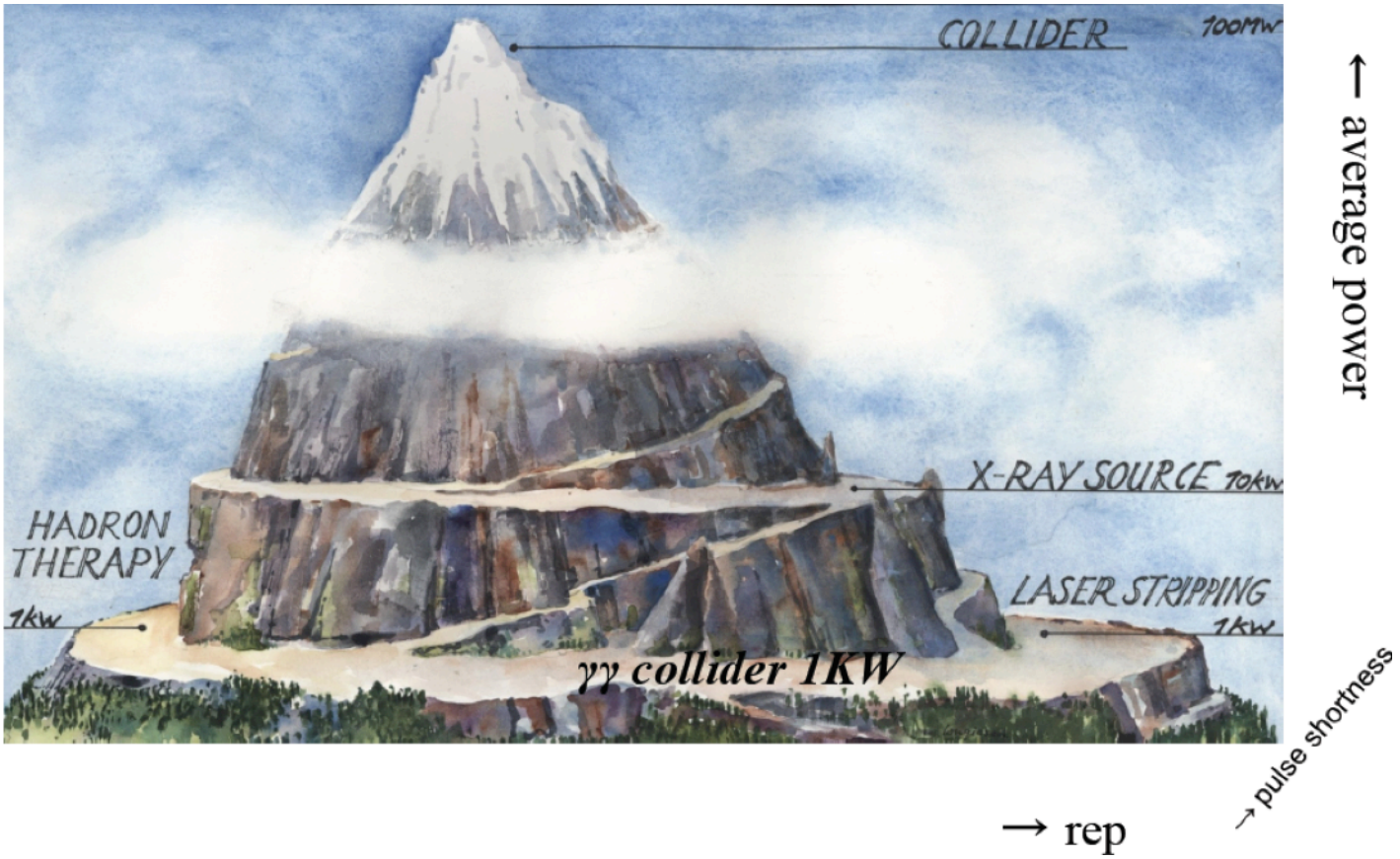

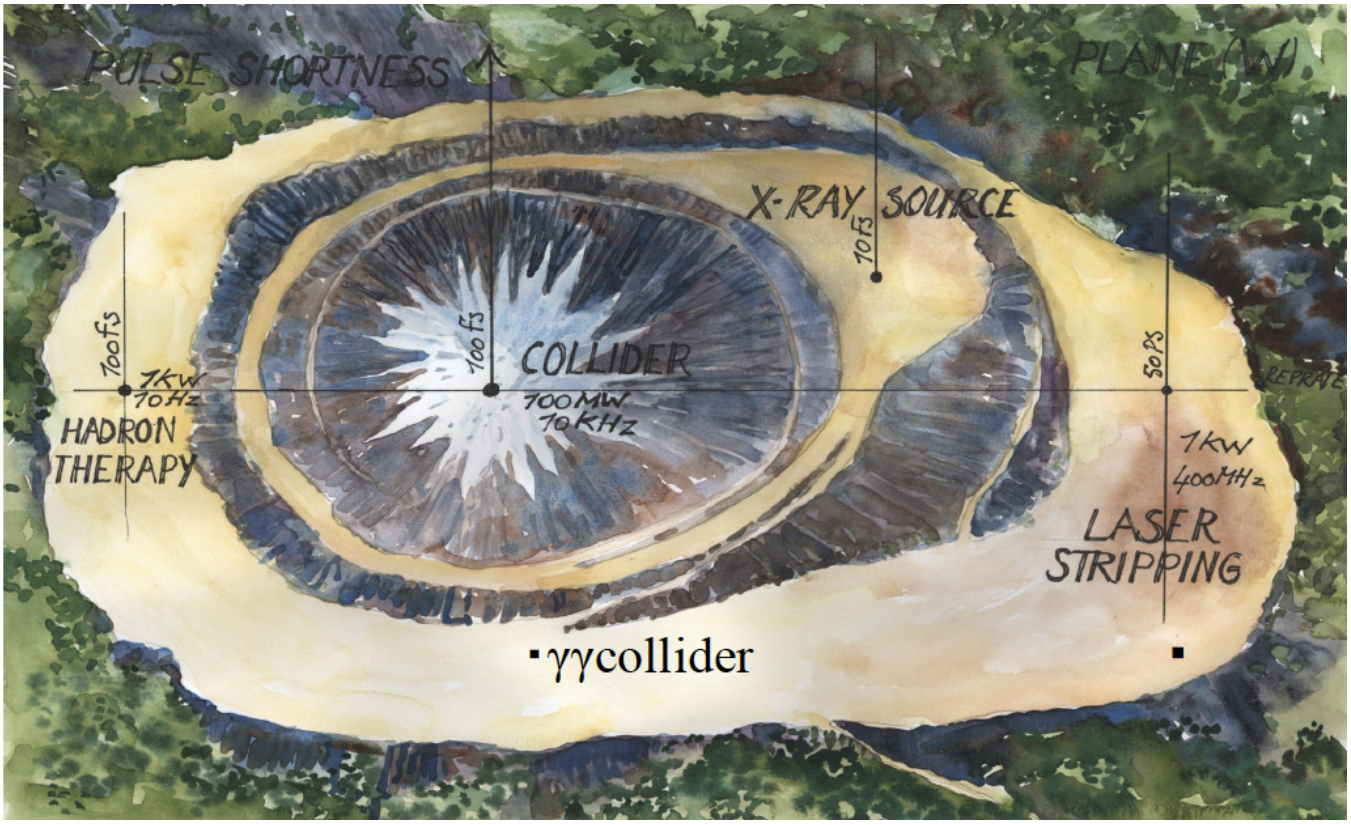

Climbing Mt. Parametrius

Shown here are more-detailed versions of the cover illustration, indicating the relative difficulty of the laser applications discussed in this whitepaper. Colliders for high-energy physics represent the presently aspirational pinnacle of laser power (*top*), but other applications are demanding in other parameters, such as short pulses and repetition rate. Illustrations courtesy T. Tajima, University of München, DE.

Contributors

Joint Task Force Members

The 2009-2011 membership of the JTF consists of members of the ICFA Beam Dynamics Panel (Ralph Assman, ICFA Beam Dynamics Panel chair Weiren Chou, Ingo Hofmann, and Kaoru Yokoya); the ICFA Advanced and Novel Accelerator Panel (Bruce Carlsten, Dino Jaroszynski, Wim Leemans, Akiro Noda, James Rosenzweig, Siegfried Schreiber and Advanced and Novel Accelerator Panel chair Mitsuru Uesaka); and ICUIL (Chris Barty, Paul Bolton, Robert Byer, Almantas Galvanauskas, Wim Leemans, and Wolfgang Sandner). Leemans is the chair of the JTF and editor-in-chief of this white paper.

Workshop Participants

In addition to the task force members, the following scientists contributed to this document: Vincent Bagnoud, Jean-Paul Chambaret, Jean-Christophe Chanteloup, John Collier, Brigitte Cros, Jay Dawson, Hartmut Eickhoff, Eric Esarey, Erhard Gaul, Erion Gjonaj, Thomas Haberer, Manuel Hegelich, Kiminori Kondo, Thomas Kuehl, Yun Liu, Matthieu Somekh, Darren Rand, Tor Raubenheimer, David Richardson, Roland Sauerbrey, Mike Seidel, Frank Stephan, Thomas Stoehlker, Toshi Tajima, Franz Tavella, Guenther Traenkle, Andreas Tuennermann, Bill White, Ingo Will, Xueqing Yan, Michalis Zervas, Bernhard Zielbauer.

Table of Contents

High Power Laser Technology for Accelerators

A joint International Committee on Future Accelerators (ICFA) and International Committee on Ultrahigh Intensity Lasers (ICUIL) whitepaper

EXECUTIVE SUMMARY

Particle accelerators, which made fundamental contributions to science and society over the last century, are poised to continue making great strides—enabled in part by remarkable recent and anticipated progress in lasers. Modern accelerators have become increasingly dependent on laser technology for a variety of uses, ranging from the production and manipulation of electron beams to novel acceleration techniques and advanced light sources. The demand for high average laser power even in near-future accelerator applications is already outpacing the state of the art in lasers. A class of more-futuristic accelerators for particle physics, driven entirely by lasers, would require average laser power far exceeding today's state of the art.

To ensure that the laser and accelerator communities understand each other's needs and to assist them in vigorous progress, the ICFA and ICUIL have set up a standing Joint Task Force, which held an international workshop.[1] The JTF identified four areas of particular interest: colliders for high-energy physics; laser stripping for H^- sources; light sources (such as x-ray free electron lasers), and medical ion therapy accelerators. That first JTF Workshop set forth the requirements for laser performance in each of these areas and assessed laser technologies that could meet these requirements, as detailed in this whitepaper.

The primary conclusion of that first Workshop was that all these applications will require progress in various laser parameters. Important aspects of the fundamental science of laser-driven accelerators have been successfully demonstrated. New proof-of-principle experiments are underway to demonstrate higher electron beam energies, to develop techniques for more control over the accelerator, and to engineer higher degrees of stability and flexible tunability. In addition to further development of the underlying accelerator technology, there is an urgent need for development of laser technology to drive future accelerators and their applications.

The following aspects of laser development were explored:

- *Power*. Improvements in average and peak power are needed for all of the application areas under consideration, especially colliders for high-energy physics. Advances in these parameters made on behalf of the accelerator community will have spinoff benefits for other uses. In turn, accelerators should benefit from laser advancements made for other purposes, though we recommend that the accelerator community should advise upon programs and steer them toward its needs, rather than hoping that these specialized and demanding needs will be addressed by others.
- *Efficiency*. To deploy and continue to advance accelerators and radiation sources, the accelerator field will need not only high average power and high peak power lasers, but also high "wall-plug" efficiency.
- *High Power Optics*. Both laser components and optics that can withstand high-average-power operation will be crucial to these advances.

---

[1] First Workshop of the Joint ICFA-ICUIL Taskforce on High Average Power Lasers for Future Accelerators, GSI (Darmstadt, Germany), April 8-10, 2010.

- *Multi-way, interactive R&D cooperation.* Engagement of the national labs, universities and industry will be essential for comprehensive R&D of new materials and new architectures for lasers, as well as for novel concepts in acceleration and radiation generation.
- *Graduate and postdoctoral education.* Innovation in accelerator and laser science and technology can be strengthened by expanding opportunities for training of students and postdocs. In some areas, better funding will be needed to bring in competition and foster stronger ties with other disciplines. Operating user facilities at national laboratories, with support for university researchers, are excellent for this.

Overall Findings

The JTF has identified several promising candidate technologies that could provide a path to the laser parameters required by future accelerator applications. A vigorous R&D program on these technology candidates is needed in the near future. The research should be guided in part by the laboratories that will benefit from each application. This collaboration between ICFA and ICUIL could play a crucial role, with the accelerator scientists providing guidance on what is needed, and the laser scientists on what is possible.

The average power and efficiency requirements of HEP applications may be met by some of these technologies after a period of development effort. Thus it is important to start a vigorous research program to start and incubate some of these technologies. Considering the size of the gap and the timing of the users' needs, it would be a long-range R&D program, perhaps five to ten years. To assess its potential, we recommend that exploratory-level research on a modest scale be started immediately.

Other applications are less demanding than colliders, but still need high average power and efficiency from their lasers. Their goals might be reached *en route* to the ultimate goal of lasers suitable for colliders, and at a much earlier date. A large scale real-world use of these interim results could provide leverage, scalability, and new technologies that are helpful in achieving the final goal.

This whitepaper is organized by application area. Discussed first are lasers in high-energy and high-intensity accelerators. Then comes a discussion of laser stripping for H^- generation in ion sources. The next chapter discusses lasers as they relate to light sources: photocathodes, FELs, etc. including Compton and Thomson scattering against an electron beam, or high-harmonic generation in gases. Laser applications in medical accelerators for proton and heavy-ion therapy are covered next. Finally a draft roadmap for laser development in support of these areas is presented, showing our vision of a long-term R&D program joining the user perspective of the accelerator community with the expertise of laser laboratories. This roadmap will be further developed in an upcoming workshop.

INTRODUCTION AND MOTIVATION

Lasers are essential to modern high performance accelerator facilities that support fundamental science and applications, and to the development of advanced accelerators. For present-day light sources they are used to drive photocathodes in high-brightness electron guns; to control and measure beam properties; and to seed the amplification process in the latest generation of light sources that rely on electron-beam-based free-electron lasers. (At the user beamlines of light sources, they are also widely used in pump-probe experiments.) In accelerator and radiation science, which aims at developing advanced acceleration and radiation source concepts, lasers provide the power for laser plasma accelerators or dielectric-structure-based direct-laser accelerators. Lasers are also used in radiation sources, such as those producing high harmonics in gases, or those producing intense gamma-ray beams via Compton or Thomson scattering against relativistic electron beams.

The performance of lasers has grown in dramatic ways, thanks to inventions such as chirped pulse amplification. Today, lasers can achieve petawatt-level peak power operating at 1 Hz; lower-energy systems (10 mJ) can operate at tens of kHz. These performance improvements have enabled a vast range of scientific opportunities, including proof-of-principle experiments on the most advanced accelerator concepts. As these laser-based techniques mature, the need for higher average power has come to the fore. Higher average power enables laboratory-tested concepts to be turned into facilities: light sources that serve a broad range of users; industrial and medical applications; or the most demanding of all, particle colliders.

Developing high average power (tens to hundreds of kilowatts), high peak power (petawatt) lasers is an extremely challenging task that will take several decades of aggressive R&D and, most likely, revolutionary new concepts and ideas.

Joint Task Force and Workshop Structure and Participation

The 2009-2011 membership of the JTF consists of members of the ICFA Beam Dynamics Panel (Ralph Assman, ICFA Beam Dynamics Panel chair Weiren Chou, Ingo Hofmann, and Kaoru Yokoya); the ICFA Advanced and Novel Accelerator Panel (Bruce Carlsten, Dino Jaroszynski, Wim Leemans, Akiro Noda, James Rosenzweig, Siegfried Schreiber and Advanced and Novel Accelerator Panel chair Mitsuru Uesaka); and ICUIL (Chris Barty, Paul Bolton, Robert Byer, Almantas Galvanauskas, Wim Leemans, and Wolfgang Sandner). Leemans is the chair of the JTF.

To understand what is needed and to plan how to build it, leading scientists from the accelerator and the laser communities convened in the First Workshop of the Joint ICFA-ICUIL Taskforce on High Average Power Lasers for Future Accelerators, GSI (Darmstadt, Germany), April 8-10, 2010. The workshop's local organizing committee was chaired by Ingo Hofmann. The workshop had 47 participants in all; they came from China (1), France (4), Germany (18), Japan (4), Switzerland (2), the UK (4) and the US (14). Accelerator experts from the collider, light source, medical accelerator, and advanced accelerator concepts communities were present. On the laser side, experts in solid state lasers, fiber laser, diode pumping, chirped pulse amplification based systems and optical components attended.

The goals of the workshop were to:

- Establish a comprehensive survey of requirements for laser-based light and particle sources, with emphasis on sources that can advance light and particle driven science, and that require lasers beyond the state of the art or at least the state-of current use. Emphasis was placed on the fact that the workshop was not intended to carry out a down-selection of specific designs or technology choices, but instead, was meant to take an inclusive approach that represents a community consensus.
- Identify future laser system requirements and key technological bottlenecks.
- From projected system requirements, provide visions for technology paths forward to reach the survey goals and outline the laser-technology R&D steps that must be undertaken.

The workshop was organized around four "work packages" by content: Colliders (led by Weiren Chou); Light Sources (led by Wim Leemans); Medical Applications (led by Mitsuru Uesaka); and Lasers (led by Chris Barty and Wolfgang Sandner).

The first day of the workshop featured plenary talks covering the different work packages, followed by discussions of the material presented. The second day was devoted to working group discussions and material development and gathering. On the third and final day, final discussions were held, followed by a summary and assignment of follow-up tasks for manuscript preparation.

The outcome of those discussions and writing assignments is this whitepaper, organized along the same lines as the work packages. The first chapter lays out requirements for lasers in future high-energy and high-intensity accelerators. Light sources and medical applications are discussed in the next three chapters. Laser technology that has the potential to provide higher average power than today's systems, and future concepts that need to be developed, are discussed in the next two chapters. The final chapter gives a summary.

Other International Workshops and Projects

Listed below are some notable examples of the emerging international dialogues and projects that bring together the laser and accelerator communities.

- *Extreme Light Infrastructure (ELI):* ELI-Beamlines (Prague) plans to provide a testbed for laser accelerators for high energy physics (on the order of 50-100 GeV). ELI-Nuclear Pillar (Bucharest) is planning an experimental facility for high energy acceleration and high energy gamma beam physics.
- *CERN* is organizing the EuCARD EuroNNAc (European Network for Novel Accelerators) to study, among other things, high energy laser wakefield accelerators. They intend to organize a pan-European and possibly worldwide network, and hosted a workshop May 3-6, 2011. This is a potential funding opportunity.
- *KEK* hosted a workshop called "Physics in Intense Fields 2010" in Tsukuba to connect the communities of fundamental physics (including particle physics/high energy physics) and intense lasers. The workshop was held Nov. 24-26, 2010, and its Proceedings have been published.
- *ILE* (L'Institut de la Lumière Extrême) organized the "Bridgelab Symposium" on Jan. 14, 2011 at L'Orme (CEA), France, to connect the accelerator labs and laser labs and to inaugurate the L'Orme lab site bridging these communities. R. Heuer, Director-General of CERN, was plenary speaker.
- ICAN (International Coherent Amplification Network) is a proposal to the European Union for the study of coherent amplification technologies for producing high average power and high efficiency that can match the collider needs. These include the fiber laser and thin disk laser technologies. Submitted to the EU last year, the project has been selected and is in budget negotiation.

1. LASER APPLICATIONS FOR FUTURE HIGH-ENERGY AND HIGH-INTENSITY ACCELERATORS

The very high gradients (~10 GeV/m) possible with laser plasma acceleration open up new avenues to even higher energy and more compact e^+e^- or muon colliders, compared to RF technology (see W. Leemans and E. Esarey, Physics Today ***62****, 44-49 (2009)). This workshop investigated the beam and laser parameters of a 1-10 TeV, 10^{36} $cm^{-2}s^{-1}$ e+e- collider based on two different technologies – laser plasma acceleration (LPA) and direct laser acceleration (DLA). The main challenges to the practical achievement of laser acceleration are: high average power (~100 MW), high repetition rate (kHz to MHz), high efficiency (~40-60%) and a cost that ideally would be an order of magnitude lower than that of RF based technology. The workshop also studied the laser requirements for a 200 GeV γγ collider, proposed as the first stage of a full scale ILC or CLIC. The required laser systems for such a collider may be within reach of today's technology.*

The consensus in the world high-energy physics community is that the next large collider after the LHC will be a TeV-scale lepton collider. Options currently under study include the ILC (0.5-1 TeV), CLIC (up to 3 TeV), and the muon collider (up to 4 TeV), all using RF technology.

The very high gradients (~10 GeV/m) possible with laser acceleration open up new avenues to reach even higher energy with more-compact machines (important because "conventional construction" and mechanical assemblies are large and costly components of such facilities). This workshop set forth a set of beam and laser parameters for a 1-10 TeV e^+e^- collider based on two different laser-based technologies – laser plasma acceleration (LPA) and direct laser acceleration (DLA).

Because the effectiveness of a collider is judged by its luminosity, and the cross section for a process creating a large mass M varies as $1/M^2$, a high-energy machine must also have high luminosity. The luminosity goal for a 10 TeV collider is 10^{36} $cm^{-2}s^{-1}$, a factor of 100 higher than for a 1 TeV machine. To reach this goal, the laser system must have high average power (~100 MW) and repetition rate (kHz to MHz).

Moreover, the laser-based collider must have high wall-plug efficiency in order to keep power consumption at a reasonable level. To set this efficiency goal, the workshop compared the efficiency of a number of large accelerators that are in an operational or a design phase. The results are listed in Table 1-1. The goal for efficiency of an LPA-based collider was set at 10%.

Table 1-1: Comparison of wall-plug efficiency of various accelerators.

Accelerator	Beam	Beam energy (GeV)	Beam power (MW)	Efficiency AC to beam	Note on AC power
PSI Cyclotron	H+	0.59	1.3	0.18	RF + magnets
SNS Linac	H^-	0.92	1.0	0.07	RF + cryo + cooling
TESLA (23.4 MV/m)	e^+/e^-	250 × 2	23	0.24	RF + cryo + cooling
ILC (31.5 MV/m)	e^+/e^-	250 × 2	21	0.16	RF + cryo + cooling
CLIC	e^+/e^-	1500 × 2	29.4	0.09	RF + cooling
LPA	e^+/e^-	500 × 2	8.4	0.10	Laser + plasma

It is difficult to set a reasonable goal for cost. Ideally, the cost should be significantly lower than that of colliders based on RF technology. Take the 0.5 TeV ILC as an example. The total estimated cost is about $8B, of which about 1/3 is the RF cost. This gives roughly $5M per GeV for RF. The laser cost of a LPA or DLA collider should be an order of magnitude lower than the RF cost of conventional colliders in order to be most attractive.

The workshop also studied the laser requirements for a 200 GeV $\gamma\gamma$ collider. This idea, originated at BINP, is interesting because the cross section for Higgs production in a $\gamma\gamma$ collider is significantly larger than that of an e^+e^- collider of the same energy. In 2008, it was proposed to ICFA to build a 180 GeV $\gamma\gamma$ collider as the first stage of a full scale ILC in order to lower the construction cost and realize a more rapid start for the project. That proposal was not approved for a number of reasons, including physics potential, cost saving potential, and the need for additional laser R&D.

This workshop concluded that the required laser systems for an ILC $\gamma\gamma$ collider may already be within reach of today's technology, whereas for a CLIC $\gamma\gamma$ collider, the required laser technology could piggyback on the inertial fusion project LIFE at LLNL or the high-power laser project ELI in Europe.

In addition to high-energy colliders, lasers also find application at another frontier–high-intensity accelerators. Lasers have been used in beam diagnostics for some time now, including "laser wire" beam profile monitoring, as well as beam polarization measurement. These require only low-power lasers. A challenge, however, is to use a laser for stripping H^- particles during injection into a high-intensity proton machine, such as the SNS, J-PARC or Project X. In these MW-scale machines, the thin foils, made of carbon or diamond, that have been used for stripping would experience a severe heating problem and have limited lifetime. Experiments have demonstrated that a laser beam interacting with H^- particles can convert them to protons. However, to replace foils in real machine operation, the laser must have high average power (kW) and high repetition rate (hundreds of MHz). This workshop investigated the required laser parameters for the SNS and Project X.

1.1. One- to Ten-TeV e^+e^- Colliders Based on Laser Plasma Acceleration

Advanced acceleration techniques are actively being pursued to expand the energy frontier of future colliders. Although the minimum energy of interest for the next lepton collider will be determined by high-energy physics experiments presently underway, it is anticipated that ≥1 TeV center-of-mass energy will be

required. The laser-plasma accelerator (LPA) is one promising technique for reducing the size and cost of future colliders—if the needed laser technology is developed. LPAs are of great interest because of their ability to sustain extremely large acceleration gradients, resulting in compact accelerating structures. *[1-3]*

1.1.1. Design principles of a LPA

Laser-plasma acceleration is realized by using a short-pulse, high-intensity laser to ponderomotively drive a large electron plasma wave or wakefield in an underdense plasma (see Figure 1-1). The electron plasma wave has relativistic phase velocity—approximately the group velocity of the laser—and can support large electric fields in the direction of propagation of the laser.

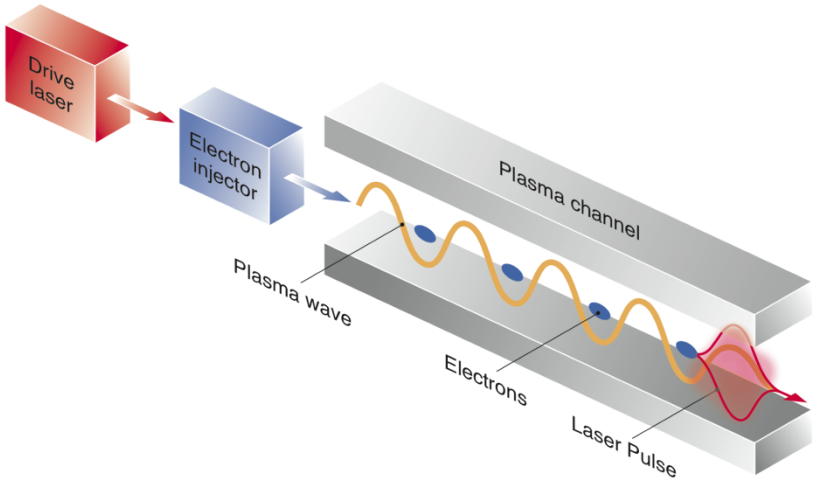

Figure 1-1: Laser-plasma acceleration: An intense laser pulse drives a plasma wave (wake) in a plasma channel, which also guides the laser pulse and prevents diffraction. Plasma background electrons that are injected with the proper phase can be accelerated and focused by the wake. *[1]*

When the laser pulse is approximately resonant (duration on the order of the plasma period), and the laser intensity is relativistic (with normalized laser vector potential $a_0 = eA/m_ec^2 \sim 1$), the magnitude of the accelerating field is on the order of $E_0[\mathrm{V/m}] = 96(n_0[\mathrm{cm^{-3}}])^{1/2}$, and the wavelength of the accelerating field is on the order of the plasma wavelength $\lambda_p[\mu\mathrm{m}] = 3.3\times10^{10}(n_0[\mathrm{cm^{-3}}])^{-1/2}$, where n_0 is the ambient electron number density. For example, $E_0 \approx 30$ GeV/m (approximately three orders of magnitude beyond conventional RF technology) and $\lambda_p \approx 100$ μm for $n_0 = 10^{17}$ cm^{-3}.

Rapid progress in laser-plasma accelerator research, and in particular the demonstration of high-quality GeV electron beams over cm-scale plasmas at Lawrence Berkeley National Laboratory, *[4]* has increased interest in laser-plasma acceleration as a path toward a compact TeV-class linear collider. *[5]* A conceptual diagram of an LPA-based collider is shown in Figure 1-2.

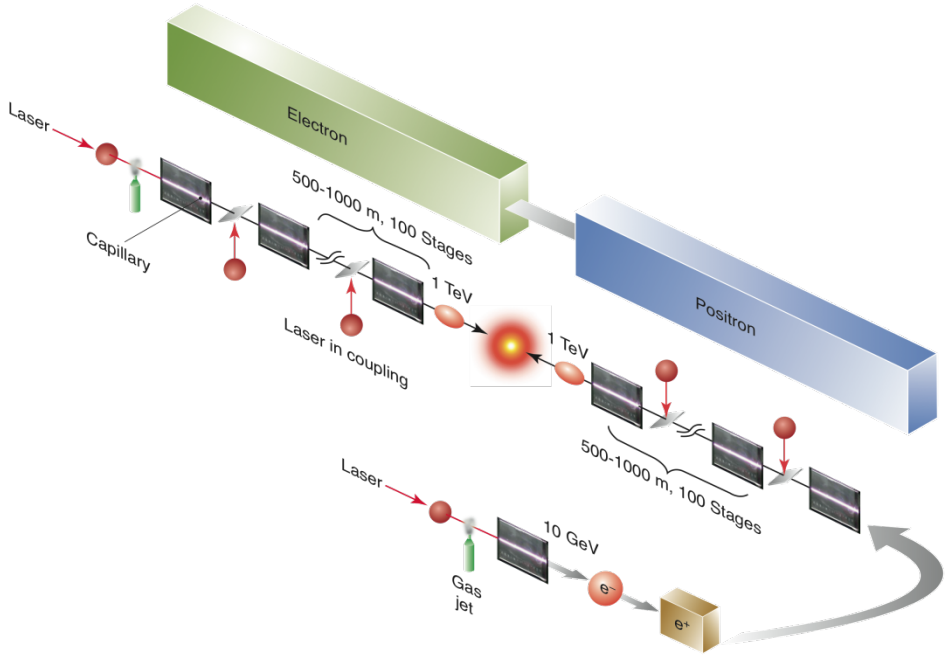

Figure 1-2: Concept for an LPA-based electron-positron collider. Both the electron and positron arms start with a plasma-based injection-acceleration module where controlled injection techniques are applied to produce a high quality ~10 GeV electron beam. Electrons are then accelerated to 1 TeV using 100 laser-plasma modules, each consisting of a 1-m long preformed plasma channel (10^{17} cm^{-3}) driven by a 30 J laser pulse giving a 10 GeV energy gain. A fresh laser pulse is injected into each module. Similarly, positrons are produced from a 10 GeV electron beam through pair creation and then trapped and accelerated in a LPA module to ~10 GeV. Subsequent LPA modules would accelerate positrons to 1 TeV. A luminosity of 10^{34} $cm^{-2}s^{-1}$ requires 4×10^{9} particles/bunch at a 13 kHz repetition rate. *[1]*

In the standard laser wakefield acceleration configuration, the electron plasma wave is driven by a nearly resonant laser (pulse duration on the order of the plasma period) propagating in a neutral, underdense ($\lambda_p >> \lambda$, where λ is the laser wavelength) plasma. There are several regimes of plasma acceleration that can be accessed with a laser driver. Two regimes that have attracted attention for collider applications are the quasi-linear regime *[3]* and the bubble *[6]* (or blow-out *[7]*) regime.

The quasi-linear regime is accessible for parameters such that $\pi^2 r_L^2 / \lambda_p^2 >> a_0^2/2\gamma_L$, where a_0^2 can be written as a function of the laser intensity I_0; $a_0^2 = 7.3\times10^{-19}(\lambda\ [\mu m])^2 I_0[W/cm^2]$ (linear polarization), $\gamma_L = (1+a_0^2/2)^{1/2}$, and r_L is the laser spot size. The amplitude of the accelerating field of the plasma wave in the quasi-linear regime is $E_z \approx 0.76(a_0^2/2\gamma_L)E_0$. This regime is characterized by regular plasma wave buckets and nearly-symmetric regions of acceleration-deacceleration and focusing-defocusing (see Figure 1-3). In the quasi-linear regime, the accelerating and focusing phase regions for electrons and positrons are symmetric, since the wakefield is approximately sinusoidal.

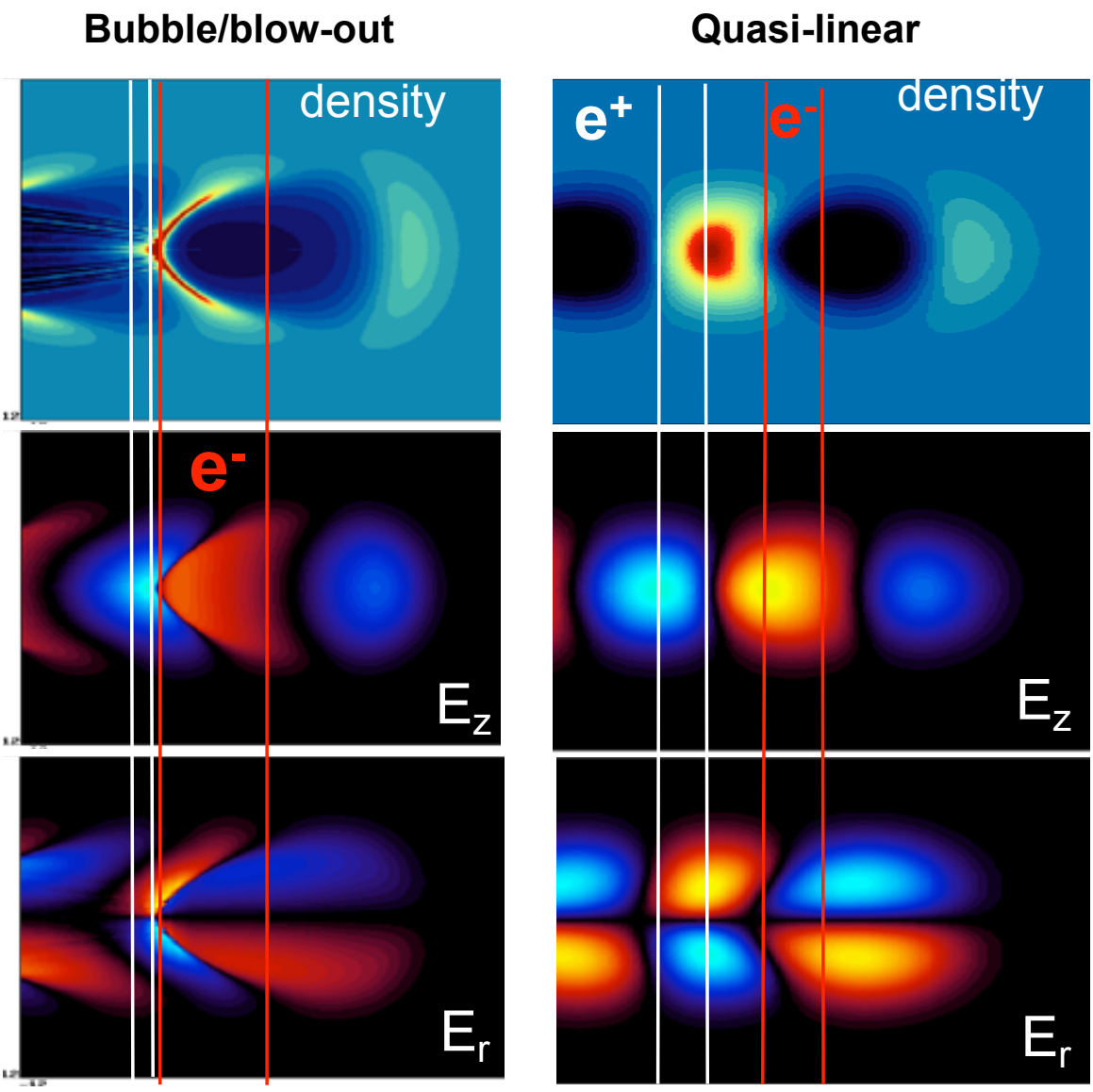

Figure 1-3: Wakes generated in the bubble (*left*) and quasi-linear (right) regimes by a laser pulse with a_0=4 (*left*) and a_0=1 (*right*). Top figures are axial electric field, central figures are density, and bottom figures are transverse electric fields. The black boxes indicate the accelerating/focusing regions for electrons, and the green boxes are for positrons. . (Courtesy C. Benedetti *et al.*, LBNL).

The bubble regime of LPA occurs for laser-plasma parameters such that $\pi^2 r_L^2 / \lambda_p^2 << a_0^2/2\gamma_L$. This regime is characterized by complete removal of plasma electrons and creation of an ion cavity (see Figure 1-3, *left*). The bubble regime has several attractive features for acceleration of electron beams. Inside the moving ion cavity, the focusing forces for electrons are linear (and attractive) and uniform for all phases and the accelerating field is independent of transverse position with respect to the cavity axis. The major drawback of the highly-nonlinear bubble regime is that acceleration of positrons is problematic because the entire ion cavity is defocusing for positrons, and a positron beam would be scattered transversely. There does exist a small phase region immediately behind the bubble where positrons could be accelerated and focused;

however, but there some of the attractive properties of the bubble regime (e.g., uniform accelerating and constant linear focusing) are lost.

The amount of charge that can be accelerated in a plasma wave is determined by the plasma density and the size of the accelerating field. The maximum charge that can be loaded—the "beam loading limit"—is given by the number of charged particles required to cancel the laser excited wake. A collider will operate with particle bunches that are asymmetric, so that the bunches can approach the beam loading limit without a large wake-induced energy spread. The maximum number of loaded charged particles into a small ($<< \lambda_p = 2\pi/k_p$) segment is approximately $N = n_0 k_p^{-3} (E_z/E_0)$.

In general, the energy gain in a single laser-plasma accelerator stage may be limited by laser diffraction effects, dephasing of the electrons with respect to the accelerating field phase velocity (approximately the laser driver group velocity), and laser energy depletion into the plasma wave. Laser diffraction effects can be mitigated by use of a plasma channel with transverse plasma density tailoring, guiding the laser over many Rayleigh ranges. Dephasing can be mitigated by longitudinal plasma density tailoring, which can maintain the position of the electron beam at a given phase of the plasma wave. Ultimately, the single-stage energy gain is determined by laser energy depletion. The energy depletion length scales as $L_d \sim \lambda_p^3/\lambda^2 \propto n_0^{-3/2}$, and the energy gain in a single stage scales with plasma density as $W_{stage} \approx E_z L_d \propto n_0^{-1}$.

After a single laser-plasma accelerating stage, the laser energy is depleted and a new laser pulse must be coupled into the plasma for further acceleration. This coupling distance is critical to determining the overall accelerator length (set by the average or geometric gradient of the main linac) and the optimal plasma density at which to operate. One major advantage of laser-driven plasma acceleration over beam-driven plasma acceleration is the potential for a short coupling distance between stages, and, therefore, the possibility of a high average (geometric) accelerating gradient and a relatively short main linac length. (Reducing the main linac length requires the coupling length between stages to be on the order of the length of a single plasma acceleration stage.) Although conventional laser optics might require meters of space to focus intense lasers into subsequent LPA stages, plasma mirrors show great promise for use as optics to direct high-intensity laser pulses, requiring only tens of cm to couple a drive laser into a plasma accelerator stage. A plasma mirror uses overdense plasma creation by the intense laser on a renewable surface (e.g., metallic tape or liquid jet) to reflect the laser beam.

The beam-beam interaction at the interaction point (IP) of a collider produces radiation (beamstrahlung) that generates background for the detectors and increases the beam energy spread, resulting in loss of measurement precision. The beam-beam interaction is characterized by the Lorentz-invariant beamstrahlung parameter Υ (mean field strength in the beam rest frame normalized to the Schwinger critical field). The current generation of linear collider designs based on conventional technology operate in the classical beamstrahlung regime $\Upsilon << 1$. Next generation linear colliders (≥1 TeV) will most likely operate in the quantum beamstrahlung regime with $\Upsilon >> 1$.

In the quantum beamstrahlung regime, the average number of emitted photons per electron scales as $n_\gamma \propto \Upsilon^{2/3}$ and the relative energy spread induced scales as $\Delta E_\gamma \propto \Upsilon^{2/3}$. Assuming that the center of mass energy, luminosity, beam power, and beam sizes are fixed, $n_\gamma \propto (N\sigma_z)^{1/3}$ and $\Delta E_\gamma \propto (N\sigma_z)^{1/3}$, where σ_z is the particle bunch length *[5]*. In this regime, beamstrahlung is reduced by using shorter bunches and smaller charge per bunch. Laser-plasma accelerators are intrinsically sources of short (fs) electron bunches, due to shortness of the plasma wavelength λ_p.

1.1.2. Parameters for a TeV class collider based on the laser-plasma accelerator (LPA)

Tables 1-2 and 1-3 show estimates of parameters for electron-positron colliders for three cases: a 1 TeV center-of-mass (CoM) collider with a plasma density of $n_0 = 10^{17}$ cm^{-3}, a 10 TeV CoM collider with a plasma density of $n_0 = 10^{17}$ cm^{-3} (Scenario I in Table 1-2), and a 10 TeV CoM collider with a plasma density of $n_0 = 10^{18}$ cm^{-3} (Scenario II in Table 1-2). In all these cases a laser wavelength of $\lambda = 1$ μm and an intensity 3×10^{18} W/cm^2 ($a_0 = 1.5$) is assumed. The laser-plasma accelerator parameters are based on scaling laws for the quasi-linear regime obtained from simulation codes. A mild plasma density taper is assumed. The length of one linac is of order of 0.1 km for the 1 TeV, $n_0 = 10^{17}$ cm^{-3} case, and of order 1 km for the 10 TeV, $n_0 = 10^{17}$ cm^{-3} case.

The conversion efficiencies assumed are 50% from laser to plasma wave and 40% from plasma wave to beam, so laser to beam efficiency is 20%. A high laser wall plug efficiency of 50% is also assumed, giving an overall efficiency, wall plug to beam, of 10%. Notice that the laser energy per stage per bunch is on the order of tens of J (for $n_0 = 10^{17}$ cm^{-3}) and the required rep rates are of the order of tens of kHz (for $n_0=10^{17}$ cm^{-3}), clearly indicating the need for the development of laser systems with high average power (hundreds of kW) and high peak power (hundreds of TW). The higher rep rate (170 kHz) and higher total wall power (3.4 GW) required for the higher plasma density case ($n_0 = 10^{18}$ cm^{-3}) is less favorable than for the $n_0 = 10^{17}$ cm^{-3} case.

A process that extracts the energy of the remaining wakefields in the plasma as well as in the bunches has been suggested.*[8]* Inserting circuitry in the plasma as a passive feedback system extracts the wakefield energy, converts this energy into electricity, and feeds it into an external circuit. The conversion efficiency is on the order of unity. Thus, it would enhance the coupling efficiency of the laser pulse to the wakefield energy by at least a factor of 2 (or even more).

Table 1-2: Beam parameters of 1 TeV and 10 TeV e^+e^- colliders based on LPA technology.

Case	**1 TeV**	**10 TeV (Scenario I)**	**10 TeV (Scenario II)**
Energy per beam (TeV)	0.5	5	5
Luminosity (10^{34} cm^{-2}s^{-1})	1.2	71.4	71.4
Electrons per bunch ($\times 10^9$)	4	4	1.3
Bunch repetition rate (kHz)	13	17	170
Horizontal emittance $\gamma\varepsilon_x$ (nm-rad)	700	200	200
Vertical emittance $\gamma\varepsilon_y$ (nm-rad)	700	200	200
β* (mm)	0.2	0.2	0.2
Horizontal beam size at IP σ^*_x (nm)	12	2	2
Vertical beam size at IP σ^*_y (nm)	12	2	2
Luminosity enhancement factor	1.04	1.35	1.2
Bunch length σ_z (μm)	1	1	1
Beamstrahlung parameter ϒ	148	8980	2800
Beamstrahlung photons per electron n_γ	1.68	3.67	2.4
Beamstrahlung energy loss δ_E (%)	30.4	48	32
Accelerating gradient (GV/m)	10	10	10
Average beam power (MW)	4.2	54	170
Wall plug to beam efficiency (%)	10	10	10
One linac length (km)	0.1	1.0	0.3

Table 1-3: Laser and plasma parameters of 1-10 TeV e^+e^- colliders based on LPA technology.

Case	**1 TeV**	**10 TeV (Scenario I)**	**10 TeV (Scenario II)**
Wavelength (μm)	1	1	1
Pulse energy/stage (J)	32	32	1
Pulse length (fs)	56	56	18
Repetition rate (kHz)	13	17	170
Peak power (TW)	240	240	24
Average laser power/stage (MW)	0.42	0.54	0.17
Energy gain/stage (GeV)	10	10	1
Stage length [LPA + in-coupling] (m)	2	2	0.06
Number of stages (one linac)	50	500	5000
Total laser power (MW)	42	540	1700
Total wall power (MW)	84	1080	3400
Laser to beam efficiency (%) [laser to wake 50% + wake to beam 40%]	20	20	20
Wall plug to laser efficiency (%)	50	50	50
Laser spot rms radius (μm)	69	69	22
Laser intensity (W/cm^2)	3×10^{18}	3×10^{18}	3×10^{18}
Laser strength parameter a_0	1.5	1.5	1.5
Plasma density (cm^{-3}), with tapering	10^{17}	10^{17}	10^{18}
Plasma wavelength (μm)	105	105	33

1.2. Ten-TeV e^+e^- Colliders Based on Direct Laser Acceleration

The Direct Laser Acceleration (DLA) research effort focuses on development of high-gradient dielectric-loaded vacuum accelerator structures driven with high-repetition-rate tabletop near-infrared lasers. The concept uses dielectric structures to couple very high laser fields to a particle beam, in much the same way that microwave structures couple RF fields to a beam, except that the wavelength and dimensions are reduced by a factor of 10,000 (from cm to μm). The dielectric structure confines a speed-of-light optical mode that is driven by a laser and will accelerate synchronous charged particles, as shown in Figure 1-4.

In contrast to plasma-coupling schemes, structure-based acceleration offers strong coupling to the particle beam, and is fundamentally a linear acceleration process. Consequently, laser pulse energies in the <1 μJ/pulse range are needed to generate GeV/m-class gradients, the process has no minimum laser energy threshold, and efficient energy transfer between laser and particle beam is possible *[9]*. Lasers with the required peak and average power, and >30% wall-plug efficiency, are commercially available. The technology to integrate much of the accelerator infrastructure onto a single silicon or silica substrate (an "accelerator chip") exists today and is being advanced rapidly by industry. The program leverages multi-billion-dollar private-sector investments in semiconductor and telecommunication technology to produce an entirely new accelerator technology.

The primary challenges for this technology are the requirement of exquisite phase control of multiple lasers and the reduction in the dimensions from microwave scales to near-IR that lead to very small machine apertures. Since carrier-phase envelope methods were proposed in 1999, significant progress in optical phase stabilization of ultrashort lasers has occurred, leading to microwave-reference frequency combs for optical metrology, and to the efficient, coherent combination of the outputs of multiple lasers *[10]*. The small apertures require constructing the accelerator structures with micron-scale dimensions. Three styles of structures are being considered: photon band-gap (PBG) fibers *[11]*, a 3-D band-gap "woodpile"' structure *[12]*, and a grating structure *[13]*. The small dimensions also require small bunch charge and small emittances, which are also naturally required by optimum beam loading and beam transport considerations. As optimum beam loading bunch charges are on the order of 10 fC, the pulse repetition rate must be dramatically raised in order to provide sufficient beam power to attain adequate luminosity. Fortunately, repetition rates in the tens of MHz range are natural for fiber lasers and allow for the bunch-by-bunch feedback systems that will be necessary to maintain beam control.

Beam transport though the small aperture requires very small normalized emittances. In a manner similar to RF accelerators, microscale periodic focusing elements will play an important role for beam containment in the structure vacuum channel. Simple beam transport considerations have led us to a possible FODO lattice for beam transport in a PBG fiber accelerator. Focusing elements of 2 cm length, 1 mm bore, and a gradient of ~500 T/m spaced ~2 m apart would allow for transport of a beam with an emittance of $\sim 10^{-10}$ m-rad through a ~1.5 λ aperture typical for these near-field structures. While 0.1 pm is a very small normalized emittance, it corresponds to a phase space density of $N/\varepsilon = 4\times10^{14}$ e/m, well below the 6×10^{15} e/m densities routinely achieved today from photo-injector sources *[14]*.

Early DLA experiments were performed on the Stanford University campus (Figure 1-5), and in 2007 the collaboration moved to SLAC and its E163 test facility in the National Linear Collider Test Accelerator (NLCTA). Recent successes include demonstration of attosecond bunch train formation *[15]* and the first demonstration of the staging of two laser accelerator sections driven at optical wavelengths. *[16]* The future program will explore the technical limits to laser acceleration, including gradient, acceptance, and emittance

preservation, and apply semiconductor and fiber-optic manufacturing techniques to demonstrate an entirely new class of structures.

Tables 1-4 and 1-5 list parameters for a 10 TeV CoM DLA collider. The intrinsically small bunch charge leads to cleaner beam collisions than any other approach considered thus far and may make the DLA technique the only reasonable choice at such very high energy.

Table 1-4: Beam parameters of a 10 TeV e^+e^- collider based on DLA technology.

Energy per beam (TeV)	5
Luminosity (10^{34} cm^{-2}s^{-1})	105
Electrons per bunch ($\times 10^9$)	0.002
Bunch repetition rate (kHz)	25000
Horizontal emittance $\gamma\varepsilon_x$ (nm-rad)	0.1
Vertical emittance $\gamma\varepsilon_y$ (nm-rad)	0.1
Horizontal beam size at IP σ^*_x (nm)	0.064
Vertical beam size at IP σ^*_y (nm)	0.064
Bunch length σ_z (μm)	335
Beamstrahlung parameter Υ	0.377
Beamstrahlung photons per electron n_γ	0.52
Beamstrahlung energy loss δ_E (%)	4.37
Accelerating gradient (GV/m)	0.5
Average beam power (MW)	39
Wall plug to beam efficiency (%)	10
One linac length (km)	10

Table 1-5: Laser parameters of a 10 TeV e^+e^- collider based on DLA technology.

Wavelength (μm)	8.0
Pulse energy/stage (nJ)	240
Pulse length (μm)	1740
Repetition rate (kHz)	25,000
Peak power (kW)	17
Average laser power/stage (kW)	10
Energy gain/stage (GeV)	1.3
Stage length [LPA + in-coupling] (m)	2.6
Number of stages (one linac)	3900
Total laser power (MW)	156
Total wall power (MW)	390
Wall plug to laser efficiency (%)	40
Laser spot rms radius (μm)	16
Laser intensity (W/cm^2)	6.4×10^9
Laser strength parameter a_0	1.2×10^{-3}

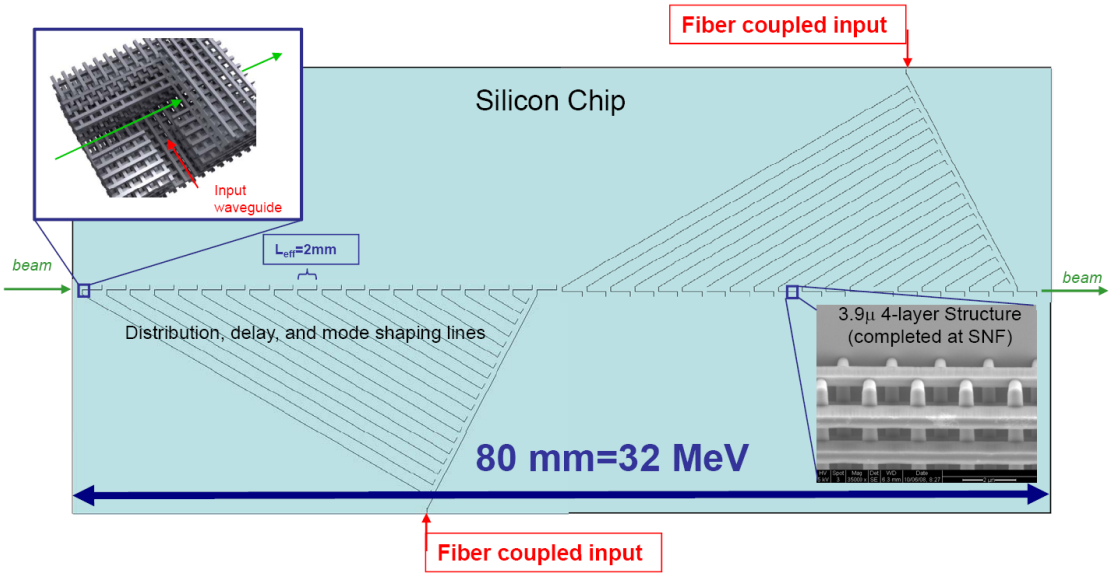

Figure 1-4: Cartoon showing an integrated silicon woodpile accelerator structure composed of 40 woodpile accelerating structures powered from two fiber lasers. At known damage fluences for 2 mm light, 32 MeV energy gain in 8 cm is expected. Cutaway of coupler region (inset, upper left, courtesy B. Cowan, Tech-X), and SEM image of fabricated silicon woodpile lattice (inset, lower right, courtesy C. McGuinness, Stanford).

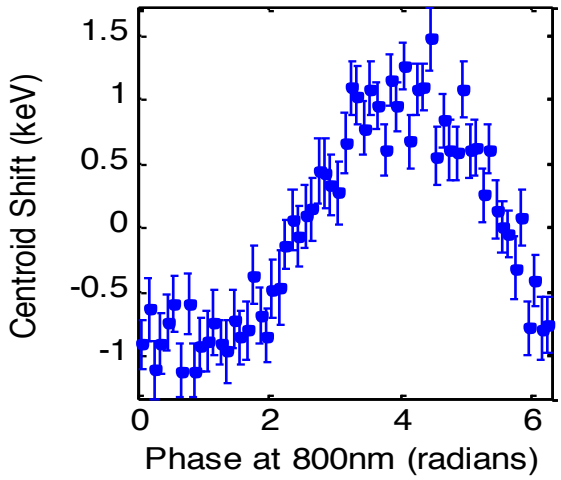

Figure 1-5: Experimental observation of optical acceleration of optically bunched electrons. The sinusoidal variation of energy of all ~350 optical bunches with the phase of the accelerator is plainly visible. Bunches are prepared by the IFEL process, and accelerated by the inverse transition radiation process. Maximum observed gradient 6 MeV/m is due to low coupling efficiency of ITR process; near-field structures are expected to yield a factor of ~100 better gradient.

1.3. Two-Hundred-GeV γγ Colliders

An electron-electron linear collider (whether RF or laser based) can be converted to a photon-photon collider by converting the electron beams into photon beams by irradiating laser beams just before the collision point as shown in Figure 1-6.

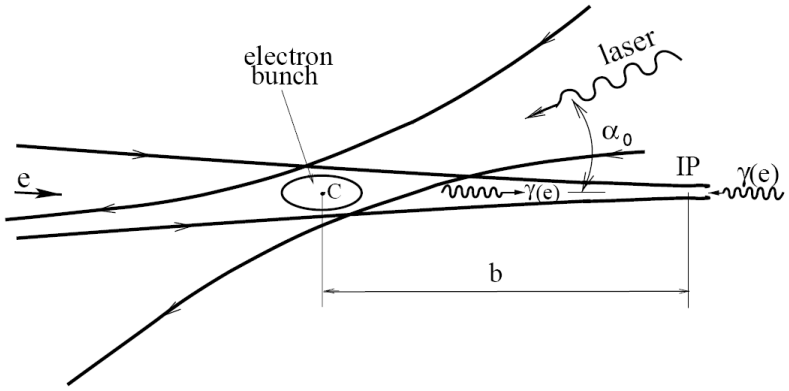

Figure 1-6: The principle of a γγ collider.

This scheme opens the possibility for investigating different physics from the collider than when it is operating with charged particle beams. The laser wavelength λ_L should be as short as possible for creating high energy photons from a given electron energy. However, it must satisfy

$$\lambda_L\,[\mu m] > \sim 4\ E_e[TeV],$$

where E_e is the electron energy, because otherwise the created high-energy photons would be lost by electron-positron pair creation in the same laser beam. To obtain a narrow photon energy spectrum, the laser beam should be circularly polarized, and the electrons longitudinally polarized. Linear polarization may sometimes be needed, depending on the physics processes being studied.

Since the transverse electron beam size at the conversion point is much smaller than the laser spot size, the probability of conversion is almost entirely determined by the laser parameters and is independent of the electron parameters as long as the electrons go through the entire length of the laser pulse. For almost all the electrons to be converted into photons, the required flash energy of the laser pulse is approximately given by

$$A = \omega_L * \sigma_C/S_L\,,$$

where ω_L is the laser photon energy, σ_C the cross section of Compton scattering, and S_L the effective cross section of the laser beam. S_L cannot be too small due to the Rayleigh length requirement. Thus, in any case A is about a few joules. On the other hand, the required pulse structure of the laser beam, which must match that of the electron beam, strongly depends on the collider design. In particular, a superconducting collider (e.g., ILC) and a normal-conducting collider (e.g., CLIC) demand very different pulse structures. The pulse structure can be characterized by a few parameters: n_b is the number of bunches in a train, t_b the interval between bunches, n_b*t_b the train length, and f_{rep} the repetition frequency of the trains. The train length is milliseconds for superconducting colliders but microseconds or less for a normal-conducting collider.

Table 1-6 shows examples of the required laser parameters for low-energy (low-mass Higgs region) γγ colliders based on the ILC and CLIC parameters. The parameters for the ILC are based on those given by V. Telnov *[17]*, slightly modified according to the present ILC parameters *[18]*. The parameters for CLIC are based on the proposal CLICHÉ *[19]* with the updated parameters of CLIC *[20]*. V. Telnov made important correction to some of the CLIC parameters as well as providing the laser parameters. *[21]* (For the ILC a possible use of an FEL is proposed *[22]* but this is irrelevant in the present context.)

All of these parameters are subject to change depending on the project evolution as well as on the optimization of the interaction region. Owing to the long bunch train (980 μs) and large bunch spacing (370 ns) for the ILC, it is possible to use an optical cavity for accumulating the laser power (the multiplication factor Q in the table) so that the requirements for the laser are greatly relaxed, at the cost of a very high precision optical system. *[23]* This type of optical cavity is similar to that currently under construction for a Compton x-ray source at KEK. *[24]*

For the CLIC it would be difficult to employ an optical cavity because the bunch train is short (177 ns) and the bunch spacing small (0.5 ns). However, the required laser system is similar to a single laser beam line of the Laser Inertial Fusion Energy (LIFE) project at LLNL in the US. This laser beam line has an output energy of >10 kJ per pulse at a repetition rate >10 Hz, or an average laser power >100 kW. (The LIFE project would need a total of 192 lines.) The amplifier can deliver a pulse of 177 ns. A modified front end can readily split a continuous pulse to 354 short pulses of 5 J each. Given appropriate funding, LLNL could put together a 10 kJ diode pumped module within 3 years. *[25]*

The main difference between LIFE and CLIC is the repetition rate (10 Hz *vs*. 50 Hz). This problem could be solved by replacing Nd:glass with ceramic Nd:YAG, which would allow the repetition rate to be increased to >50 Hz. Technology similar to this has also been proposed for the Extreme Light Infrastructure (ELI) project in Europe. *[26]*

Table 1-6: Beam and laser parameters of γγ colliders.

Electron Beam Parameters	**ILC**	**CLIC**
Energy per electron beam (GeV)	100	100
Max energy of photons (GeV)	60 (75)	60
γγ luminosity at the high energy peak (10^{34} cm^{-2}s^{-1})	0.13	0.19
Electrons per bunch (× 10^{10})	2	0.68
Number of bunches in a train (n_b)	2640	354
Distance between bunches (t_b, ns)	370	0.5
Length of the train (n_b*t_b , μs)	980	0.177
Repetition frequency ($f_{rep,}$ Hz)	5	50
Electron bunch length σ_z (μm)	300	44
Normalized emittance $\varepsilon_{x/y}$ (mm-mrad)	10/0.035	1.4/0.050
Beta-function at IP $\beta_{x/y}$ (mm)	4/0.3	2/0.02
Beam size $\sigma_{x/y}$ (nm)	450/7.3	120/2.3
Distance between conversion point and IP (mm)	~1.5	~0.5
Crossing angle (mrad)	25	25
Laser Parameters		
Wavelength (μm)	1 (0.5)	1
Rayleigh range (mm), f#	~0.5, 20	~0.4,18
Laser pulse energy (J)	~10/Q	5
Pulse length (r.m.s., ps)	~1.5	~1
Peak power (TW)	~2.5/Q	2
Average power (kW)	150/Q	90
Laser power in a train (MW)	25/Q	10000
Cavity enhancement factor	Q~300	1

Notes on Table 1-6 (by V. Telnov):

1) Distance between the Compton conversion point (CP) and the interaction point (IP) is $b = \gamma\sigma_{y.}$
2) Thickness of the laser target is equal to 1.2 collision lengths.
3) Luminosity in the high energy peak means $L_{\gamma\gamma}(W > 0.8W_{max})$
4) For the ILC, the numbers are given for $\lambda = 1$ μm. Those in ( ) are for $\lambda = 0.5$ μm.
5) For the ILC, $\lambda = 1$ μm is OK and $\lambda = 0.5$ μm may be possible. But for CLIC only $\lambda = 1$ μm is allowed because the disruption angle is 1.5 times larger. [The disruption angle is proportional to $(N/\sigma_z)^{1/2}$.]
6) "Undulator" parameter $\xi^2 = 0.15$ (0.2) was used for $\lambda = 1$ (0.5) μm, corresponding to reduction of W_{max} by 5%.

Chapter 1 References

1. W.P. Leemans and E. Esarey, *Physics Today* **62**, 44 (2009).
2. T. Tajima and J.M. Dawson, *Phys. Rev. Lett.* **43**, 267 (1979).
3. E. Esarey, C.B., Schroeder, W.P. Leemans, *Rev. Modern Phys.* **81**, 1229 (2009).
4. W.P. Leemans *et al*., *Nature Physics* **2**, 696 (2006).

5. Schroeder, C.B., E. Esarey, C.G.R. Geddes, C. Benedetti, and W.P. Leemans, "Physics considerations for laser-plasma linear colliders," Phys. Rev. ST Accel. Beams 13, 101301 (2010).
6. Pukhov and J. Meyer-ter-Vehn, *Appl. Phys.* **B 74**, 355 (2002).
7. W. Lu et al., *Phys. Rev. ST Accel. Beams* **10**, 061301 (2007).
8. T. Tajima and A. Chao, private communication; also Wu, H. C., Tajima, T., Habs, D., Chao, A., and Meyer-ter-Vehn, J., *Collective deceleration: toward a compact beam dump*, Phys. Rev. STAB **13**, 101303 (2010).
9. R. H. Siemann, "Energy efficiency of laser driven, structure based accelerators", *Phys. Rev. ST Accel. Beams* **7**, 061303, (2004); see also N. Na, *et al.*, "Energy efficiency of an intracavity coupled, laser-driven linear accelerator pumped by an external laser", *Phys. Rev. ST Accel. Beams* **8**, 031301 (2005).
10. W. Liang, A. Yariv, A. Kewitsch, G. Rakuljic, "Coherent combination of semiconductor lasers using optical phase-lock loops", *Opt. Lett*., **32** (4), p. 370 (2007).
11. X. E. Lin, "Photonic band gap accelerator", *Phys. Rev. ST Accel. Beams* **4**, 051301, (2001).
12. B. Cowan, "Three-dimensional dielectric photonic crystal structure for laser-driven acceleration", *Phys. Rev. ST Accel. Beams* **11**, 011301, (2008); see also C. McGuinness *et al.*, "Accelerating electrons with lasers and photonic crystals", *J. Modern Optics*, **56** (18&19), p. 2142ff (2009).
13. T. Plettner *et al.*, "Proposed few optical cycle laser driven particle accelerator structure", *Phys. Rev. ST Accel. Beams* **9**, 111301, (2006); see also T. Plettner, R.L. Byer, "Proposed dielectric-based microstructure laser-driven undulator," *Phys. Rev. ST Accel. Beams* **11**, 030704 (2008).
14. E. Colby *et al*., "An electron source for a laser accelerator", *in Proc. 2003 Part. Accel. Conf*., p. 2101-2103 (2003).
15. C.M.S. Sears *et al.*, "Production and characterization of attosecond bunch trains", *Phys. Rev. ST Accel. Beams*, **11**, 061301 (2008).
16. C. M. S. Sears *et al.*, "Phase stable net acceleration of electrons from a two-stage optical accelerator", *Phys. Rev. ST Accel. Beams*, **11**, 101301 (2008).
17. Private communication.
18. http://www.linearcollider.org/about/Publications/Reference-Design-Report
19. D. Asner *et.al*., "Higgs physics with a γγ collider based on CLIC 1", *Eur. Phys. J. C* **28**, 27–44 (2003)
20. R. Tomas, "Overview of the Compact Linear Collider", *Phys. Rev. ST Accel. Beams* **13**, 014801 (2010). Two parameter sets for $E_{CM} = 0.5$ and 3 TeV are given. Here, the former is used.
21. Private communication.
22. For example, E. Saldin *et al*., Proc. PAC2009, Vancouver, BC, Canada, WE6PFP083.
23. For example, G. Klemz *et al*., "Design study of an optical cavity for a future photon collider at ILC", *Nucl. Instr. Meth*. **A564**, 212 (2006).
24. J. Urakawa, "Development of a compact x-ray source based on Compton scattering using 1.3 GHz superconducting RF accelerating linac and a new laser storage cavity", submitted to *Nucl. Instr. Meth*. A.
25. C. Barty, private communication.
26. W. Sandner, private communication.

2. LASER STRIPPING OF H^- PARTICLES IN HIGH-INTENSITY PROTON ACCELERATORS

Lasers have great potential usefulness for stripping H^- particles into without the need for foils (e.g., in "beam stacking" for a Spallation Neutron Source power upgrade); for production of ions through photoionization; and for achieving higher ionization states.

2.1. Laser Stripping of H^- Particles for SNS

The Spallation Neutron Source (SNS) utilizes charge-exchange injection to "stack" a high-intensity proton beam in the accumulator ring for short-pulse neutron production. In this process, a 1 ms long H^- beam pulse is transported to a carbon stripping foil located at the injection point of the ring. The electrons are stripped and the resulting proton beam is merged with previously accumulated beam. This injection scheme is central to the operation of many facilities, including the SNS, J-PARC, ISIS and PSR.

As the beam power of the SNS is increased from the 1.44 MW design to more than 3 MW as envisioned in the SNS Power Upgrade project, the stripping foils become radioactive and produce uncontrolled beam loss, which is one of the main factors limiting beam power in high intensity proton rings.

A "foil-less" charge exchange injection method was first proposed in the 1980s by using a field dissociation process. This scheme requires an impractically large laser power, which is indeed the central difficulty involved in ionizing neutral hydrogen. Recently, ORNL scientists came up with a three-step scheme for laser stripping.

An H^- ion has two electrons. The first electron is loosely bound with a binding energy of 0.7 eV, whereas the second one is tightly bound with a binding energy of 13.6 eV. The ORNL 3-step scheme works as follows. First, H^- ions are converted to H^0 by stripping off the first electron in a magnetic field; then H^0 atoms are excited from the ground state ($n = 1$) to the upper levels ($n \geq 3$) by a laser, and the excited states H^{0*} are converted to H^+ by stripping the second electron in a second magnetic field.

In a proof-of-principle experiment, a third harmonic beam from a Q-switched laser was used for stripping. The laser generates a 30 Hz, 6 ns pulses with a peak power of ~10 MW at 355 nm. The stripping efficiency reached 90%. The positive result has encouraged us to proceed in developing a real scheme for SNS stripping. Such a system will need to reach an efficiency of 98%, similar to that of conventional foils.

A simple multiplication of 10 MW laser peak power, used in the first experiments, and the duty factor of the SNS beam (6%), yields an average laser power of 0.6 MW at 355 nm to strip the entire ion beam. Obviously, this power is impractical. Therefore, a number of approaches have been investigated to mitigate the requirement of peak/average laser power.

1) Optimization of H^- beam parameters

   An appropriate dispersion derivative of the H^- beam will be designed to eliminate the Doppler broadening of the absorption line width and therefore to reduce the required frequency sweep for the laser beam. The vertical size as well as the horizontal angular spread of the H^- beam will be minimized. The optimization of the H^- beam parameters will reduce required peak power of the laser to the 1 MW level. Reduction of the bunch length of the ion beam can further reduce the average laser power requirement.

2) Macropulse laser system

   At SNS, the H^- beam consists of approximately 50-ps long micropulses separated by ~2.5 ns and gated into mini-pulses 650 ns long. The period of minipulses, or a turn, is determined by the SNS accumulation ring beam path length (~1 μs) and the beam energy. The minipulses are bunched into macropulses with a length of 1 ms and a repetition rate of 60 Hz. In order to achieve high efficiency laser stripping, the laser pulses need to overlap with each ion beam micropulse at the interaction point. The ideal (minimum laser power requirement) condition would be that the laser pulses have an identical temporal structure as the H^- beam. A prototype of such a macropulse laser system has been developed in collaboration with Continuum Inc. It includes a mode-locked seed laser, a pulse picker, multi-stage solid-state amplifiers, and harmonic generation crystals to convert infrared beam to UV light. The challenges of the macropulse laser system are the high repetition rate and macropulse duration.

3) Beam recycling optical resonator

   The photon-hydrogen interaction results in a negligible loss to the laser beam power; it is expected that the average power of the laser can be significantly reduced by recycling the laser beam with an optical resonator. Different cavity configurations including Fabry-Perot, ring cavity, or cavity with built-in harmonic generation crystals need to be investigated. Optical resonator technology is well developed for low-power, infrared, and often continuous laser beams. However, for the SNS the resonator needs to work on a high intensity UV laser beam. In addition, since the photon-hydrogen interaction has to occur inside the resonator, the optics need to operate within a high vacuum, and its control electronics need to survive a high radiation dose. These constraints pose severe technical challenges in the development of the optical resonator.

Table 2-1 lists the parameters of the SNS H^- beam and Table 2-2 summarizes the required laser parameters with and without the beam recycling optical resonator.

Table 2-1: SNS H^- beam parameters.

Beam energy (GeV)	1.0 (upgrade: 1.3)
Beam power (MW)	1.4 (upgrade: 3.0)
Beam macropulse length (ms)	1.0
Beam micropulse length (ps)	50
Peak macropulse H- current (mA)	38
Ring accumulation time (turn)	1060
Ring bunch intensity	1.6×10^{14}
Vertical size (mm)	0.6
Vertical emittance (mm-mrad)	0.225π
Horizontal size (mm)	3
Vertical emittance (mm-mrad)	0.225π

Table 2-2: Required laser parameters for SNS laser stripping.

Method	**Macropulse laser**	**Macropulse laser w/ 20× resonator**
Laser wavelength (nm)	355	355
Micropulse length (ps)	50	50
Micropulse energy (μJ)	50	2.5
Micropulse repetition rate (MHz)	402.5	402.5
Macropulse length (ms)	1	1
Macropulse energy (J)	20	1
Macropulse repetition rate (Hz)	60	60
Average power (W)	1200	60
Temporal profile	Flat	Flat
Contrast	N/A	N/A
Efficiency	Normal solid-state lasers	Normal solid-state lasers
Polarization	100/1	100/1
Cost	Multi $M	Multi $M
Laser beam quality	$M^2 < 1.2$	$M^2 < 1.2$
Pulse stability	1%	1%
Laser pointing stability (μrad)	1	1
Laser availability	24/7	24/7

2.2. Laser Stripping of H^- Particles for Project X

Project X at Femilab would convert H^- particles to protons at 8 GeV. Laser stripping would be easier here than in SNS because a laser of longer wavelength could be used—the photon energy would be increased by the relativistic γ factor (γ = 9.526) due to the Doppler shift. The beam parameters are listed in Table 2-3 and the beam pulse structure is shown in Figure 2-1.

Table 2-3: Project X H^- beam parameters.

Kinetic energy (GeV)	8
Relativistic γ	9.526
Micropulse length (ps)	15 ps
Micropulse frequency (MHz)	325
Micropulse period (ns)	3.1
Macropulse length (ms)	1.25
Macropulse current (mA)	20
Macropulse frequency (Hz)	5
No. H^- per micropulse	4×10^8
No. micropulses per macropulse	4×10^5
No. H^- per macropulse	1.6×10^{14}
No. H^- per second	8×10^{14}
Vertical beam size (mm)	1.5
Horizontal beam size (mm)	1.5
Beam power (MW)	1

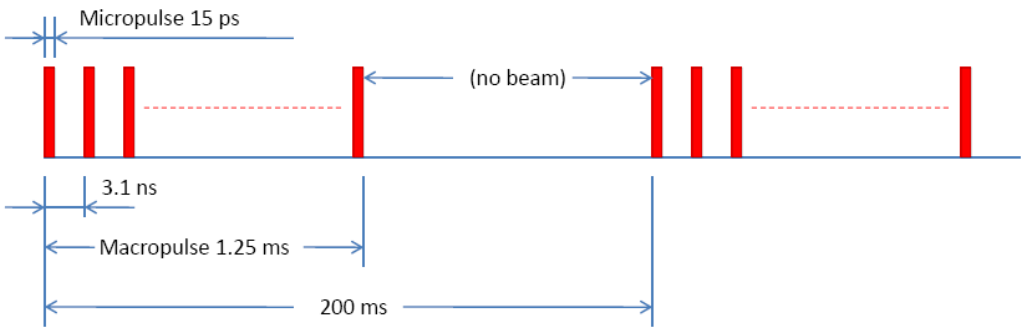

Figure 2-1: H^- pulse structure of Project X.

2.3. Direct Laser Ionization

Besides their usefulness for stripping particles emitted by an ion source, lasers can also be used to cause ionization.

The photoionization of the ground state of the hydrogen atom H(1s) has been studied extensively in the past half century. For low-intensity radiation, there are exact expressions of this process in terms of the cross section obtained from the perturbation theory. *[27]* In this approximation, the incident photon flux density is much smaller than 1 atomic unit (a.u.) and the pulse duration is much longer than an optical cycle. However, this approximation is no longer valid when intense laser pulses are employed, since the peak electric fields can be comparable with or larger than 1 a.u. and the pulse may last only a few optical cycles or even a fraction of a cycle. Therefore, perturbative methods are not applicable, and numerical methods for solving the time-dependent Schrödinger equation (TDSE) are required.

Ionization of hydrogen atoms by intense laser pulses is a complex subject that is still not fully understood. *[28-30]* Although many theoretical approaches have been proposed, they typically break down at high laser intensities or neglect important aspects of the laser-atom interaction, such as long-range Coulomb interaction or realistic pulse shapes. Numerical solutions of the TDSE provide accurate predictions, but are extremely computationally intensive and converge slowly at high intensities. Current results show that no simple relationship links ionization rate to pulse duration, frequency and intensity, due to competing ionization mechanisms, evolving energy levels, resonances and stabilization.

Calculations performed for 24.8 nm (50 eV), 2.5 fs (30 periods) pulses suggest that intensities beyond 10^{17} W/cm^2 are required for efficient (>90%) ionization of hydrogen atoms. *[31]* From an experimental standpoint, few absolute measurements of the ionization yield are available. An experiment performed with 600-fs, 248-nm laser pulses measured ~0.001% ionization for intensities of the order of 10^{14} W/cm^2 . *[32]*

2.4. Three-Step Stripping

Electrons in hydrogen atoms exposed to intense laser radiation can be excited to higher states. For the Project X parameters, the n = 2 transition can be triggered when the hydrogen beam interacts with a 1024 nm laser beam at an angle of ~96°. A laser peak power of ~3.5 MW is required for 90% stripping.

It may be possible to reduce the required laser energy by decreasing the incidence angle (Figure 2-8). However, this approach can only be investigated by performing detailed simulations of the response of hydrogen atoms to the laser field.

Counter-propagating geometry would require a laser at around 1.8 μm, which could be achieved using an OPA. However, detailed calculations would be required to establish the powers required and the role of Stark shifting, etc.

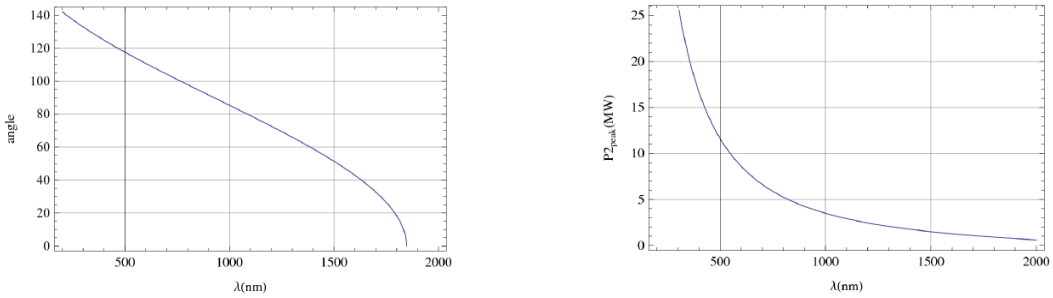

Figure 2-8: Wavelength *vs.* angle and power *vs.* wavelength required for ionization of hydrogen atoms.

Chapter 2 References

27. H. A. Bethe and E. E. Salpeter, *Quantum Mechanics of One- and Two-Electron Atoms*, pp 295-322, Springer-Verlag (1957).
28. A. N. Grum-Grzhimailo *et al*., *Phys. Rev.* **A 81**, 043408 (2010).
29. S. Borbély *et al*., *Phys. Rev.* **A 77**, 033412 (2008).
30. S. Geltman, *J. Phys. B: At. Mol. Opt. Phys*. **33**, 1967 (2000).
31. J. Bauer *et al*., *J. Phys. B: At. Mol. Opt. Phys*. **34**, 2245 (2001).
32. G. A. Kyrala and T. D. Nichols, *Phys. Rev.* **A 44**, R1450–R1453 (1991).

3. LIGHT SOURCES

This section discusses the requirements on performance for lasers that are used in conjunction with RF accelerators; drivers for laser plasma accelerators that in turn power a free electron laser or other advanced radiation source; and for Thomson scattering based gamma-ray sources.

Lasers already play a significant role in existing light source facilities, but face new challenges with future light sources that aim at much higher repetition rates. Ultrafast (femtosecond) lasers reaching 1-10 kW levels will be required for seeding and user driven experiments. Lasers producing a few joules in 30-50 fs pulses at high repetition rate (100-1000 Hz) could be used to drive laser plasma accelerator. Thanks to their ability to produce GeV-class, ultra-short, high peak current electron bunches, these laser plasma accelerators could in turn drive compact free electron lasers operating in the soft x-ray regime. Higher energy per pulse lasers (~40 J) would be needed to drive multi-GeV electron bunches for hard-x-ray FELs.

3.1. Lasers for RF Accelerator Based Light Sources

Lasers are widely used in today's RF accelerator based light sources. Uses range from photocathode gun based linacs; to phase space manipulation (heating) or diagnosis of electron beams; seeding FELs with high harmonics from gases, liquids or solids; and user experiments on high-repetition-rate facilities.

3.1.1. Guns and heaters

The requirements for photocathode laser systems are different for various current and future light sources, mainly depending on the time structure of the electron beam and the photocathode material. The time structure parameters range from low-duty-cycle, single-shot schemes via microbunch trains (burst mode laser systems) to CW operation. The photocathode materials can be various metals or different types of semiconductors, and thus wavelength requirements can range from the UV (e.g., copper and Cs_2Te) to green (e.g., alkali antimonite). The laser system has to be synchronized to the RF system with a precision of a small fraction of a degree of the specific RF phase, and almost all projects require temporal and spatial laser pulse shaping.

Besides the requirements for high power laser systems for burst mode and CW operation, two additional fields of research have been identified: 3D ellipsoidal shaping of the laser pulses, and alternative cathode material developments.

A key parameter to extend the performance of short wavelength light sources is transverse emittance, which must be reduced. This quantity has a cathode dependent lower limit (thermal emitttance). Space charge and RF curvature can cause further emittance growth. To minimize these other sources of emittance growth, 3D ellipsoidal shaping is promising: simulations for a 1 nC bunch showed a > 25% reduction of the projected emittance and >10% reduction of the central slice emittance, in comparison to an optimized "beer can" laser pulse shape.

Smaller transverse emittance will extend the scientific reach of short wavelength FELs by, e.g., lasing at even shorter wavelengths; allowing saturation at lower beam energy or with shorter undulators; two-color lasing; and higher levels of transverse coherence at lower beam energies. In addition, the longitudinal phase space is very linear, enabling smoother bunch compression. At low bunch charges, very short electron bunches can be produced, allowing longitudinally coherent FEL laser pulses (single spike lasing). This

shaping will also reduce the beam halo, reducing the radiation damage to undulator segments and diagnostics components.

Table 3-1 summarizes the laser requirements of photocathode systems.

Table 3-1. FEL photocathode laser systems requirements. Powers listed assume a factor of 10× for overhead associated with spatial and temporal shaping as well as transport losses. Yellow indicates that some further development is needed; red indicates a need for significant R&D.

Type	Wavelength	Pulse energy	Pulse duration	Rep rate	Peak power	Average Power	Comment
Yb fiber	Tunable, frequency doubled to 475–558 nm on cathode	0.5–90 nJ green 5–700 nJ IR	1–50 ps (FWHM)	Up to 1 MHz	1.8 kW green 14 kW IR	0.1 W green 0.8 W IR	Photocathode laser for alkali antimonide cathodes. Temporal and spatial pulse shaping, and synchronization are required.
IR quadrupled	200 nm on cathode	100 nJ UV	1–50 ps(FWHM)	Up to 1 MHz	2 kW UV	0.1 W UV 10s W IR	Photocathode laser for cesium telluride cathodes. Temporal and spatial pulse shaping, and synchronization are required.
IR quadrupled	260 nm	20nJ – 1uJ	20 ps	180 kHz – 9 MHz		2 W UV	Photocathode drive for CW Euro-XFEL
IR quadrupled	260 nm on cathode	10 uJ UV	20 ps (FWHM)	Up to 5 MHz burst	500 kW UV	50 W UV burst 3 W avg 500 W IR burst	5 MHz burst mode for 0.6 ms
IR Doubled	510-532 nm on cathode	100 nJ Green	10 ps(FWHM)	Up to 1.3 GHz	10 kW Green	130 W Green 500-1000 W IR	For future ERL upgrades to 1.3 GHz

Another important field of research is the study of different cathode materials. Besides the usual aim of high quantum efficiency at manageable vacuum requirements, cathode development has goals that include:

- Lowering the power requirements and simplifying the photocathode laser system if high quantum efficiency photoemission at longer wavelength (green spectral range) can be used.
- Improving the usability of different cathode materials in superconducting RF cavities. Besides heat deposition by the photocathode laser beam, the RF joint with the cavity and the compatibility with high gradient SC cavities are issues.
- Reducing the thermal emittance. Since the solid state properties of the photocathode also determine the thermal emittance for given laser spot size, a proper choice of cathode material will have increasing proportional importance when the other sources of emittance are reduced further and further.

Laser heater systems are needed in many facilities for increasing the uncorrelated momentum spread of the electron beam from photocathode RF guns (Table 3-2). Usually, though, they can rely on the residual IR radiation from the photocathode drive laser system.

Table 3-2. Laser systems requirements for the heater laser of an FEL laser.

Type	Wavelength	Pulse energy	Pulse duration	Rep rate	Peak power	Average power	Comment
IR	800 nm	~10 μJ	50 ps (FWHM)	1 MHz	200 kW	10 W	Residual IR from drive laser is typically suitable

.

3.1.2. FEL seeding

Today's EUV, soft X-ray and hard X-ray free electron lasers are based on the self-amplified spontaneous emission (SASE) principle. While this is a very robust mode of operation, it makes it difficult to generate photon pulse properties tailored to scientific user needs in terms of defined pulse shape and length, longitudinal coherence, and timing stability. The drawbacks in FEL beam quality mainly stem from the SASE process starting up from shot noise, which results in considerable spectral and energy fluctuations.

Seeding the amplification process with external radiation rather than shot noise is a promising method to increase the spectral brilliance and to achieve pulses that are stable in frequency spectrum and in energy. The output power of the seeded FEL is concentrated in a single line, which is many times narrower than the spectrum of the conventional SASE FEL (Fig. 3-1).

External seeding also makes it possible to synchronize the seeded FEL pulse with an additional pump-probe laser system to better than the pulse length, which is typically 10 fs or less. Synchronization to the fs level opens a wide field for revolutionary ultra-fast physics experiments. Such novel synchronization schemes are being developed at FLASH, Fermi@Elettra *[33, 34]* and other places. These systems are based on compact ultra-stable fiber laser systems providing a timing reference. Synchronization systems are not yet mature and need considerable R&D.

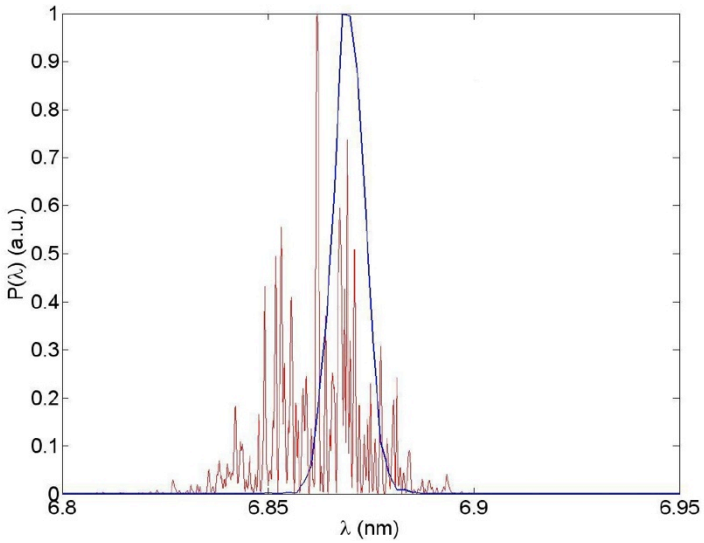

Figure 3-1: Typical wavelength spectral distribution of a single SASE FEL pulse. Red: calculated for a typical SASE process starting from shot noise. Blue: with external seeding.

Seeding of the amplification process by an external laser pulse has been considered for a long time and was demonstrated in a proof-of-principle experiment at SCSS/Japan. *[35]* Seeding improves the FEL beam properties considerably and thus extends the range of possible applications. A method of producing the seed radiation is the generation of higher harmonics (HHG) from near-infrared femtosecond laser pulses in rare gas media. *[36, 37]* Odd harmonics of the laser fundamental are created and used as seeding radiation pulses.

Beyond fundamental issues in the realization of seeding at VUV and X-ray wavelengths, it is particularly challenging to realize a femtosecond laser system for very short pulse lengths. The minimum pulse duration is determined by the bandwidth of the FEL gain process, resulting in a natural coherence time of approximately 4 fs at VUV wavelengths (at FLASH, for example) and below 1 fs at X-ray wavelengths. The seed pulse should be shorter than the electron bunch, thus increasing the impact of longitudinal slippage effects. As an example, simulations show that a seed energy of a few nJ (or 50 kW peak power) with >1 eV bandwidth is required at FLASH to seed a wavelength of 7 nm.

Due to the low conversion efficiency of the HHG process (~10^{-6} to 10^{-8}) and transport losses, the energy of the external laser pulse has to be at least 5 mJ, which means close to 1 TW peak power. These power levels are particularly problematic at high rep rates, where the resultant average power is hundreds to thousands of watts. Methods for enhancement of higher order harmonic generation process (i.e., quasi-phase-matching) should also be considered as a possibility to reduce the energy requirements for the driver laser.

Table 3-3 shows the parameters for future fourth generation light sources and Table 3-4 shows the respective seed-laser parameters for cw FELs and burst mode FELs. To name an example, a prototype beyond-state-of-the-art seed laser is being developed for FLASH. At present, several tens of μJs at 7 fs are achieved with a repetition rate of 100 kHz. In the near future, an upgrade to 1 to 3 mJ per pulse as required for the HHG seeding process is planned. *[38]*.

Other methods of seeding are multiplication techniques like high gain harmonic generation HGHG *[39]*, echo-enhanced harmonic generation EEHG *[40]* and various other combinations. *[41]* It has also proposed to use FEL based lasers for self-seeding approaches. *[42]* Since it is not at all obvious which of the seeding

options will be the most efficient and cost effective path forward, and the answer may even vary from machine to machine, experiments are scheduled.

For high average brilliance FELs like burst-mode FELs (FLASH *[43]* and the European XFEL *[44]*); cw FEL proposals (NGLS *[45]* and NLS [46]); or Energy Recovery Linacs (Cornell ERL *[47]*, BerlinPro *[48]*), average laser power would have to be in the kW range. As an example, a repetition rate of 1 MHz asks for a seed laser with an average power of 5 kW. Repetition rates beyond 1 MHz, e.g., 4.5 MHz for the European XFEL, or 1 GHz for the ERL upgrade proposals) need considerable R&D, as they are beyond the reach of present technology. The main problems to be solved are similar in all high power lasers: the removal of heat together with the need for efficient pumping schemes (e.g., for optical parametric chirped amplification).

Table 3-3: Parameters of a Future FEL Source.

Type	High rep-rate seeded FEL facility (CW SCRF Linac)
E (GeV)	2.5
I (mA)	1
ε_x (ε_y) (mm-mrad)	$\leq$ 0.8 (norm.)
Spectral peak (keV)	1
Peak brightness (ph/s/mm^2/mrad^2 /0.1%BW @spectral peak)	10^{29}–10^{33} (depends on FEL configuration)
Average brightness (ph/s/mm^2 /mrad^2 /0.1%BW @spectral peak)	10^{18}–10^{26}(depends on FEL configuration)
Average flux (ph/s)	10^{13}–10^{17}
Average coherent flux (ph/s)	~ full coherence
Photons/ pulse	10^{8}–10^{12}
Charge/bunch (pC)	10–1000
Beam pulses per second	10^{6}
Beam pulse length	~100 fs
Machine size C or L (m)	700
Cost & Schedule	$ 1B; 10-year construction
Comment	LBNL design concept

Table 3-4: FEL Seed Laser and User Systems Requirements. Yellow indicates that some further development is needed; red indicates a need for significant R&D.

Type	Wave-length	Pulse energy	Pulse duration	Rep rate	Peak power	Average power	Comment
IR drive w/ multiplication	800 nm quadrupled to 200 nm	~10s μJ UV and IR both required	few cycle IR to ~100s fs(FWHM)	10–100 kHz	Up to GW	~1 W UV ~10s W IR	EEHG UV and IR both required at electron bunch CEP stabilization required for ultrafast pulses
IR drive w/ multiplication	200 nm Tunable at the electron bunch	~10s μJ UV	10 –100s fs (FWHM)	10–100 kHz	~100 MW	~1 W UV ~10s W IR	HGHG
IR drive Direct	IR drive laser 30 nm to e bunch	~5 nJ @ 30 nm	~10–50 fs(FWHM)	10–100 kHz	100 kW (@ 30 nm)	500 μW (@ 30 nm) ~500 W IR	HHG - CEP stabilization required for ultrafast pulses
IR drive Direct Burst	IR drive laser 4-40 nm to electron bunch	~5-50 nJ @ 4-40 nm	~5–50 fs (FWHM)	5 MHz Burst	100-1000 kW	50 kW IR 200W avg	HHG - CEP stabilization required for ultrafast pulses
IR drive Direct	IR drive laser 30 nm to electron bunch	~5 nJ @ 30 nm	~10–50 fs (FWHM)	1 MHz	100 kW (@ 30 nm)	5000 μW (@ 30 nm) ~5 kW IR	HHG - CEP stabilization required for ultrafast pulses
IR drive Direct Solids	IR drive laser 1 nm to electron bunch	~5-500 nJ @ 1 nm	~10–50 fs (FWHM)	10–100 Hz	1 PW IR	.1 - 1 kW IR	Relativistic harmonics from solids

3.1.3. Lasers for Users

Users of light sources will typically require optical lasers in conjunction with the light source beam to either pump or probe matter. Because many of these experiments will be investigating matter on time scales of the light source x-ray pulses, conventional lasers will need to provide short pulses at the rep-rate of the light source. These conventional pulses will need to be energetic enough to excite states in matter to be probed by the x-rays and will need to have flexibility in wavelength that allows pumping and probing of as many states as possible. In general, this implies tens of mJ of laser energy with pulse widths that range from

<10 fs to picoseconds. Such a laser should also be compatible with harmonic conversion, as well as with pumping of optical parametric amplifiers (OPAs).

Pumping and probing of matter with the x-ray source and a conventional laser implicitly requires a high degree of synchronicity between the light source and the optical laser. Pushing this synchronicity to levels better than 1 ps will require non-conventional (most likely optical) timing distribution systems. Even with timing distribution systems capable of sub-picosecond drift and jitter, the inherent jitter in many of the light sources will require diagnostics that can measure the relative arrival times of the optical laser and the light source or electron bunch at the femtosecond level. In this case, the data can be post-processed with the temporal resolution of the measurement of the relative arrival times.

3.2. Lasers for Laser Plasma Accelerator Driven FELs

In 2006, a cm-scale laser plasma accelerator powered by a 40 TW laser pulse (2.3 J/pulse) produced a 1 GeV electron beam with a time integrated energy spread of about 2.4%, containing 30 pC of charge. Currently, experiments are underway at many institutions to demonstrate that such beams are capable of powering an FEL. Using a conventional undulator with cm-scale period, beams of just a few hundreds of MeV would be sufficient to produce extreme ultra-violet radiation in the 5-30 nm range. Production of shorter wavelength radiation in the soft x-ray regime (1-5 nm) would require beams with energy on the order of a few GeV which could be produced from an LPA by somewhat increasing the length of the accelerator structure, reducing the plasma density, and using laser pulses with 5 J/pulse. Harder x-rays would require yet higher laser pulse energy (order 10-30 J) in 100 fs pulses, and plasma structures with length on the order of 50-80 cm and densities of order $1\text{-}2\text{x}10^{17}$ cm^{-3}.

The applicability of this technology for user facilities would require repetition rates that are beyond state-of-the-art of today's high peak power lasers. Operating an FEL at 1-10 kHz would require lasers with average power in the 1-10 kW range for soft x-ray FELs and reaching towards 100 kW for hard x-ray FELs.

Typical parameters are listed in Table 3-5.

Table 3-5. Laser Requirements for Laser Plasma Accelerator Driven FELs. Red shading indicates areas where significant further R&D is needed.

Type	Wave-length	Pulse energy	Pulse duration	Rep rate	Peak power	Average power	Wall plug efficiency	Comment
Mode locking laser oscillator	1 μm	50 mJ	10 ps (FWHM)	162.5 MHz or 81.25 MHz	5 GW	8125 kW or 4062.5 kW	50% (if successful by using fiber laser)	Using self-starting laser amplification with super-optical cavity, a technology developed by Y. Honda, K. Sakaue and H. Shimizu. Demonstration of average stored power > 500 kW this year.
Fiber laser	1.03 μm	1.25 μJ in FP cavity ~ 30 mJ	1 ps	160 MHz	1.25 MW	200 W	~ 40%	TDR phase
MOPA	1 um	10 J	1-100 ps	1 kHz	.1 – 10 TW	10 kW	>10%	Also a pump laser for below
MOPA	.8	2-3 J	< 50 fs	1 kHz	40-60 TW	2-3 kW	?	LBNL Laser driven source Scattering laser as above
MOPA	.8	15 J	5 fs	10 Hz	3 PW	150 W	?	Relativistic mirror for coherent keV production Needs extreme contrast ratio

3.3. Thomson Scattering Sources for Gamma-Ray Production

Thomson scattering can provide a wide variety of novel x-ray sources with unprecedented properties. They are likely to allow for a new dimension of ultra-fast medical and material diagnostics, and to revolutionize remote material analysis, ultrahigh-resolution scattering microscopy and holography. There are two classes of proposed working schemes: those using conventional electron accelerators or storage rings as a scattering target, and pure laser schemes, with laser backscattering from laser-accelerated electron beams**.** Besides classical Thomson backscattering, a novel method exploiting massive "piston"-type acceleration with ultra-high intensities (exceeding 10^{20} W/cm^2) holds the promise of truly coherent x-ray sources. Table 3-6 gives the parameters of Thomson sources.

3.3.1. Incoherent hard x-rays

Development of compact monoenergetic MeV gamma sources could allow special nuclear materials (SNM) signatures to be obtained with greatly reduced radiation doses to the target, compared to broadband bremsstrahlung sources, and allow increased standoff distance. Narrow energy spread also reduces background, which could improve nuclear resonance fluorescence (NRF) signatures. Thomson scattering of laser photons from relativistic electrons produces suitable narrow bandwidth gamma-rays and has been

demonstrated on conventional linacs. Electron beams at 200-800 MeV energies can produce photons at 1.7 - 15 MeV suitable for NRF or photofission interrogation and mrad divergence for remote detection at a standoff range of hundreds of meters. A 300 MeV electron beam with 10^9 electrons and 2% energy spread (similar to what has been achieved in recent experiments), scattering with a 40 J, ps laser, could produce ~$3x10^8$ gammas at 1.7 MeV matched to the U-235 NRF, with a few-% energy spread and mrad divergence. Electrons at ~700 MeV would access photofission.

Several projects for accelerator-based Thomson x-ray sources have been started worldwide.

Table 3-6. Parameters of Thomson sources. Red shading indicates areas where significant further R&D is needed.

Type	**E** (MeV)	**Energy Spread (%)**	**I** (mA)	**Spectral peak** (keV)	**Peak brightness** (ph/s/mm^2/mrad^2 /0.1%BW	**Average flux** (ph/s)	**Photons/ pulse**	**Charge/ bunch** (pC)	**Pulses /s**	**Pulse length**	**Cost & schedule**
Compact high-brightness X-ray Source **(Linac)**	20-50		50	0.2-70	$>10^{17}$	$>10^{12}$	$>10^{11}$	200	5	1 ms	$ 5M; five-year R&D to be completed by 31/03/2013
ThomX **(Ring)**	50		20	47	varying	10^{12-13}	5×10^5	1000	2×10^7	1-20 ps	€ 5.5M; 3-4 years
Conventional Compact gamma source	500-1000	10^{-3}		1000 - 15000	1.5×10^{21}	$>10^{12}$					TBD
Laser Compact gamma source	500-1000		.1uA	1000 - 15000	$>10^{23}$	$>10^{12}$	$>10^9$	.1 – 1 nC	**1000**	**1-5 fs**	TBD

Laser plasma accelerators (LPAs) produce electron beams with percent energy spread at the required 0.2–1 GeV energies in 0.2–3 cm [4,5]. Hence LPAs have the potential to reduce the size of SNM gamma sources by orders of magnitude. In LPAs , the radiation pressure of a laser drives a space-charge wave, or wake, in a plasma producing the high gradient . They also produce fs bunches and may be used for other radiation sources including free electron lasers. A project at LBNL is given as an example.

Although Thomson backscattering can, in principle, work with any kind of laser sources, optimal performance in terms of photons per pulse, brightness and average output intensity requires both a high pulse energy and a high repetition rate. In the case of linear accelerator driven devices, where the bunch cycles are of high frequency, pulse energies in the range of 50 mJ at a repetition rate of 81.25 MHz—or, better, 162.5 MHz—would be a good choice. This seems feasible using fiber lasers, with a typically very good efficiency. The specific case of a storage ring device can benefit from a large resonator cavity along the interaction section, thus reducing the laser power demand by 4 orders of magnitude.

To produce electrons in the GeV range, laser plasma acceleration experiments have demonstrated the need for peak power of the order of 50 TW. High average power operation requires repetition rates on the order of one kHz or more. In order to reach average output intensities similar to the accelerator driven sources with their higher repetition rate, the backscattering laser has to produce a pulse energy of 10 J with 1- to 100-ps pulse duration. A laser of this class has similar performance to the pump laser required for an OPA-laser solution for the laser-acceleration driver.

3.3.2. Future coherent hard x-ray sources

A novel and yet not well explored alternative to the above sources, at least for the photon energy range of 10 – 100 keV, is proposed in the "relativistic mirror" concept. Assuming an acceleration of a thin foil by laser pressure, an electron "piston" with critical density can be generated, moving at relativistic speed. Backscattering from this electron layer, in contrast to Thomson scattering, is expected to affect every single photon of the backscattering laser. The specific problem of this approach is the ultra-high intensity level of > 10^{21} W/cm^2 needed to reach the piston regime, and the ultra-high contrast requirement needed to establish a clean interaction process. The development of such ultra-high contrast petawatt sources is, however, an important demand of many other applications of lasers accelerators. Parameters for these lasers are also given in the above table.

Chapter 3 References

1. S. Schulz, L. Wissmann, J. Zemella, M. K. Bock, M. Felber, P. Gessler, F. Ludwig, K.-H. Matthiesen, H. Schlarb, B. Schmidt, F. Loehl, V. Arsov, A. Winter, "All-optical synchronization of distributed laser systems at FLASH" Proceedings of PAC09, Vancouver, BC, Canada, TH6REP091.
2. Fermi@Elettra, Conceptual Design Report, elettra-trieste website.
3. G. Lambert, T. Hara, D. Garzella, T. Tanikawa, M. Labat, B. Carre, H. Kitamura, T. Shintake, M. Bougeard, S. Inoue, Y. Tanaka, P. Salieres, H. Merdji, O. Chubar, O. Gobert, K. Tahara AND M.-E. Couprie, "Injection of harmonics generated in gas in a free-electron laser providing intense and coherent extreme-ultraviolet light", Nature Phys. **4**, 296 (2008).
4. J.G. Eden, "High-order harmonic generation and other intense optical field-matter interactions: review of recent experimental and theoretical advances", Progress in Quant. Elec. 28, 197-246 (2004)
5. J. Seres, E. Seres, A.J. Verhoef, G. Tempea, C. Streli, P. Wobrauschek, V. Yakovlev, A. Scrinzi, C. Spielmann and F. Krausz, "Source of coherent kiloelectronvolt Xrays", Nature **433**, 596 (2005).
6. F. Tavella et al., Opt. Express **5**, 4689-4694 (2010).
7. L.-H. Yu, et al., Science **289**, 932 (2000).
8. G. Stupakov, "Using the beam-echo effect for generation of short-wavelength radiation", Phys. Rev. Letters 2009, 102: 074801.
9. C. Feng, Z.T. Zhao, "Hard X-ray free-electron laser based on echo-enabled staged harmonic generation scheme", Chinese Sc. Bull. **55** (2010), 221–227.
10. J. Feldhaus, E.L. Saldin, J.R. Schneider, E.A. Schneidmiller, and M.V. Yurkov, Opt. Commun. **140**, 341 (1997).
11. W. Ackermann et al., "Operation of a free-electron laser from the extreme ultraviolet to the water window"; Nature Photonics **1**, 336 - 342 (2007)
12. European XFEL, technical design report (http://xfel.desy.de/tdr/)
13. Next Generation Light Source, LBNL website (http://www.lbl.gov/LBL-Programs/ngls/science/index.html - internal only)
14. New light source (NLS) project, http://www.newlightsource.org
15. J. A. Crittenden, "Developments for Cornell's X-Ray ERL", Proc. PAC 2009, Vancouver, BC, Canada, MO4PBC03.
16. P. Kuske, "The BERLINPro Project", Proc. ESLS XVI, Daresbury, UK, Nov. 2008.

4. MEDICAL APPLICATIONS: PROTON/CARBON THERAPY

Laser acceleration of protons/ions has the potential to replace current technology used in tumor therapy. Such lasers are typically very high peak power (PW class) and require special pulse shapes with very high temporal contrast. Compact lasers with multi-kW average power will be needed.

The medical application of laser ion acceleration is discussed here in the context of ion beam therapy with protons or carbon beams. Worldwide the most common approach to radiation therapy is with photon beams (x-rays generated by electron accelerators), which benefit from the affordable cost and compact size of the device. The advantage of ion beams lies in the Bragg peak that is characteristic of how protons and heavy ions are stopped by matter—they deposit most of their energy across a short distance near the end of their range—which allows predominant and peaked irradiation in depth at the position of the tumor while sparing healthy tissue. This unique radiobiological advantage of protons (and, even more, of carbon beams) is evidenced by the success of ion beam therapy in former and existing facilities (Berkeley, Chiba, GSI, and the recently completed Heidelberg Ion Therapy facility).

These facilities, with combined use of proton and carbon beams, rely on conventional accelerator technology, where a linear accelerator is used as the injector for a synchrotron. This technology has been developed to extremely high efficiency due to 3D scanning techniques in irradiation and proven high reliability (up to 98%). Facilities using protons alone are realized cost-effectively by compact cyclotrons.

Among the drawbacks of synchrotrons are their large size and cost, which limit this approach to larger hospitals with three to five treatment rooms. The potential for using laser acceleration instead of a linac and synchrotron may be seen in significantly reduced system size and cost, and might offer further advantages (facilitating gantry design, for example).

The most recently built HIT facility is used here as a reference for state-of-the-art performance and cost. We assume that maximum flexibility is desired to enable treatment of small as well as large in-depth tumor volumes requiring the maximum energy of 250 MeV for protons and 400 MeV/u for carbon. We adopt their reference numbers for the required total number of protons / carbon ions per fraction (5 min) as well as peak numbers (per second) in a spot-scanning delivery mode. Other parameters (like energy spread and total number of voxels) are adjusted to the particularities of laser acceleration, which include a much higher production energy spread than in the synchrotron case and a laser pulse rate suggested by current technology.

Table 4-1 lists the laser parameters for various medical accelerator applications.

4.1. Ion Beam Parameters for Medical Applications

4.1.1. Ion beam production: laser and target parameters

The laser acceleration of ions provides many orders of magnitude more acceleration gradient than conventional acceleration, on the order of 1 TeV/m. Energetic proton and ion beams with high beam quality have been produced in the last few years from thick metallic foils (e.g., few-μm-thick aluminum) irradiated by ultra-intense short laser pulses.

The results from most previous experiments have been based on the Target Normal Sheath Acceleration (TNSA) model. As these targets are relatively thick, the laser pulse is mostly reflected and the conversion efficiency of laser energy to ion energy is normally less than 1%. The dependence of maximum ion energy upon laser intensity is less than a linear function. The maximum proton energy based on the TNSA mechanism has improved little since the year 2000 (~68 MeV, the cutoff energy for the exponential spectrum).

Because of the advantage in accelerating limited mass, experiments producing high-energy ions from sub-micrometer to nanometer targets much thinner than the ones in early experiments, and driven by ultrahigh contrast (UHC) short-pulse lasers, have attracted strong interest recently. There are two key issues:

1) Generation of quasi-monoenergetic ion beams by reduction of intrinsic energy spread.

2) Accelerating protons to 250 MeV, or C^{6+} ions to 400 MeV per nucleon via laser foil interaction.

The possibility of accelerating quasi-monoenergetic ion bunches has already been demonstrated within the TNSA regime by restricting the ion source to a small volume, where the sheath field is homogenous. However, a very high laser intensity of $>10^{22}$ W/cm^2 is required in order to accelerate protons to above 200 MeV. A new mechanism for laser-driven ion acceleration was proposed, where particles gain energy directly from the Radiation Pressure Acceleration or Phase Stable Acceleration (RPA / PSA). By choosing the laser intensity, target thickness, and density such that the radiation pressure equals the restoring force established by the charge separation field, the ions can be bunched in a phase-stable way and efficiently accelerated to a higher energy.

In proof-of-principle experiments, quasi-monoenergetic peaks for C^{6+} at ~30 MeV were observed at MPQ/MBI and C^{6+} at >500 MeV (exponential) and 100 MeV (quasi-monoenergetic) was observed at LANL. Furthermore at LANL, quasi-monoenergetic protons at ~40 MeV were generated from thin (nm) diamond-like carbon foils. Theoretical study shows that the required medical proton beams can be generated from hydrogen with a laser intensity of $\sim 10^{21}$ W/cm^2, and medical carbon beams can be generated from carbon foils of submicron thickness with a laser intensity of 10^{22}W/cm^2.

4.1.2. Ion beam quality to treatment area

The distance from the skin to the deepest tumors in the body determines the required particle energy. From the stopping range in water, the necessary acceleration energy for reaching deep tumors is 400 MeV/u for carbon and 250 MeV for protons. The number of ions is defined by the dose requirements for killing cancer cells. Referring to HIT data, the necessary total number per fraction is estimated to be $\sim 2.5\times10^9$ for carbon, and $\sim 1\times10^{11}$ for protons. With reference to the ongoing hadron therapy schedule, the exposure time in HIT is usually below 5 minutes, which we have adopted for the laser case. For spot-scanning delivery, each fraction is irradiated in units of "voxels" (volume elements) with a pulse reproducibility of better than 5%. Using a 10 Hz laser system, a maximum of 3000 voxels can be irradiated in 5 minutes.

The number of ions needed per voxel varies strongly from shot to shot, and is highest in the distal layer. This defines the maximum number of ions needed per shot at the top energy. For a standard 2 Gy dose, and an assumed 1 cm^2 voxel area, is estimated to be ~2×10^7 for carbon, and ~7×10^8 for protons. Then the maximum ion irradiation rate at the top energy is ~2×10^8 ions/s for carbon and 7×10^9 particles/s for protons, which means that the maximum beam power at the tumor is ~0.2 W for carbon and 0.4 W for protons. These numbers must be compatible with the maximum beam power at the laser target (ion source). In the proton case, 10^{10} protons per shot (10^{11} per second) should be possible, which corresponds to 4 W (and hence a significant overproduction to be eliminated by absorbers for a quasi-monoenergetic beam at 250 MeV).

Ion beam treatment also requires a sufficiently high beam quality (small emittance and controlled energy spread) to realize a scanning technique. In principle, the 6D phase space density of the laser accelerated beam is extremely high due to the very small production spot radius (~5-10 μm) and the very short production time interval (~100 fs). The actual beam quality in the subsequent transport and focusing structure is, however, not primarily a function of the production phase space density, but of what can be maintained in the particle collection and transport. It can be shown that the predominant factor determining transverse emittance is chromatic aberration of a collector lens. The achievable beam quality for an assumed energy spread of ± 5-10% for SOBP (spread-out Bragg peak) is, however, still consistent with chromatic aberrations of a high-field solenoid collector lens.

Based on this, a typical number of energy steps of scanning in the longitudinal direction is 5 to 10. At the top energies (for reaching the distal edge of the tumor) the energy spread probably needs to be smaller to minimize irradiation of healthy tissue beyond the tumor.

In this report, for the purpose of estimating specifications for future laser systems, we assume a large tumor. However, for treatment of much smaller, very early stage tumors, the required number of ions can be significantly reduced, as well as the required range of energies. We can use current or future imaging resolution limits to estimate the minimum tumor size that can be located and treated. In this case some laser specifications might also be lower, and even present technology might allows developing a therapy system for animal tests. Also, for such small tumors, spot-scanning is less likely to be an appropriate delivery mode.

4.1.3 Reproducibility and reliability

For irradiating tumor cells, very high reproducibility and reliability are required. In the event of an overexposure, the ion beam would deposit the excess energy into healthy cells surrounding the tumor. The total dose should be controlled with a high accuracy—to within plus or minus a few percent. In this sense, by increasing the shot rate, we can reduce the total dose error resulting from shot-to-shot dose fluctuation. The beam reproducibility for each voxel should be better than 5%, as is already described. The accuracy of delivered dose per voxel becomes critical in cases where each voxel is irradiated by only one proton bunch from one laser shot (or a few in the case of rescanning or "repainting"). Of course, the total dose accuracy depends on the cancer type. It is also essential to address the tumor motion problem (attributed to breathing, patient positioning and other organ motion, for example). In this case, the total dose error is thought to be within ± 20% at present. For regular predictable motion such as that caused by respiration, this is typically done with gated irradiation. However, spot-scanning beam delivery combined with tumor tracking can be more efficient and is under development.

Table 4-1: Parameters of Laser Acceleration for Medical Applications (assuming spot-scanning delivery)

Parameter	**HIT (proton/carbon)**	**laser proton**	**laser carbon**
Comments:	synchrotron based; slow extraction	RPA, SOBP	
Energy of ions (MeV)	250/400	250	400
Ions per 5-minute fraction	~ 1×10^{11} / 2.5×10^{9} (5 min)	~ 1×10^{11} (5 min)	~ 2.5×10^{9}
Voxels per fraction	Typically 20k	3k (300 sec x 10 Hz)	
Laser rep rate (Hz)		10	10
Max. ions per 1 cm^2 voxel ($\times10^8$) needed for 2 Gy dose in distal layer	Usually lower due to smaller voxels	7	0.2
Max. ions per second ($\times10^8$) for spot scanning over distal layer		70	2
Energy steps	~ 50	5-10	
Energy spread	<0.005	±0.05 (less at distal layer)	
Bunch/laser repetition rate (Hz)		10	
Emittances (mm-mrad) (before window)	2-3	~ 20-50 (depending on transport distance)	
Max ion beam power on tumor (W)	0.16	~ 0.16	~ 0.8
Max production power (W)	~ 0.16	~ 4 (10^{10} p/shot) (target dependent)	(no numbers)

4.2 Requirements for Lasers

The laser requirements (Table 4-2) are driven first and foremost by the particle energy requirement of hadron therapy, i.e., 250 MeV for protons and ~ 400 MeV/nucleon for carbon. Achieving these energies will probably require laser acceleration of ions in the Radiation Pressure Acceleration (RPA), Phase Stability Acceleration (PSA), or Break-out Acceleration (BOA) regimes. Ion energies achievable in the TNSA regime do not scale favorably with laser intensity, and the spectral yields from the targets are typically quasi-exponential (as opposed to quasi-monoenergetic).

While intensities beyond 10^{22} W/cm^2 are required to reach the desired carbon energies, simulations indicate that the 250 MeV proton energy might be accessible at 10^{21} W/cm^2 with optimum targets. However, the optimal target thickness depends on laser intensity, and it is very hard to make a thin, cryogenic liquid or solid hydrogen target (which will be required for efficient proton acceleration); therefore the actual optimal intensity for a proton machine might be on the same order of magnitude as for carbon.

Due to the nature of the target—very thin but of very high (solid) density—laser intensity contrast is a key requirement, as shown in the table below. These conditions are imperative and cannot be reduced.

While the optimum laser pulse duration remains unclear, these newer acceleration mechanisms have been demonstrated at 45 fs and 500 fs. It is clear from both experiments and simulations that pulses with fast rise time are necessary for highest efficiency, stable acceleration, and a quasi-monoenergetic spectrum. We propose a rise time of ≤20 fs.

A flat-topped transverse pulse profile in the focal plane is another requirement that will require R&D.

Altogether, those requirements equate to an energy on target, within a 5 μm radius and with a flat top focus, of 150 J in the proton case and 1500 J in the carbon case. For therapy applications those parameters must be obtained at a 10 Hz rep rate and with ≤1% stability. For use in hospitals, a compact laser that is part of a compact "integrated laser-driven ion accelerator system" (ILDIAS) will be of great value. The overall accelerator system has to include space for imaging and spatial filtering devices, a transport beamline with appropriate instrumentation, and a sophisticated beam delivery subsystem for treatment.

Minimizing the laser pulse energy requirement would contribute significantly to minimizing the cost of the overall facility. Ultrashort pulse durations would facilitate reaching the high range of laser intensity that is of interest. The required dose rate should be reached with a minimum repetition rate of 10 Hz.

With the laser approach it might be possible to reduce cost by reducing the shielding requirements for radiation protection and by reducing gantry size. The cost of the building and of the gantry represents about 50% of the total cost in conventional hadron therapy centers. This part might be reduced by an estimated factor of 5. Further, more-quantitative assessment of these issues is required. The cost of the laser acceleration unit itself (the ILDIAS) should probably be between 10-15 M€ in order to remain competitive with the total cost of a single-treatment-room proton cyclotron facility, which is currently about 20 M€.

Table 4-2: Laser parameters.

Parameter	laser proton	laser carbon
Laser repetition rate (Hz)	10	
Laser pulse energy (J)	150	1500
Average power (kW)	1.5	15
Pulse duration (fs)	50-150	
Peak power (PW)	1-3	10-30
Intensity (W/cm^2)	1-3x10^{21}	1-3x10^{22}
Laser wavelength (nm)	800-1054	
Spot radius mp	5 (flat)	
Contrast (at 5 ps/500 ps)	$10^{-8}/10^{-12}$	$10^{-9}/10^{-13}$
Pulse rise time (fs)	<20	
Efficiency	1-10%	
Polarization	lp/cp	
Laser beam quality	diffraction limit	
Pulse stability	0.01	
Laser pointing (maser) [master? –jc]	1-10	
Laser availability	12 h/day (50% duty factor)	
Failure rate	<2%	

5. LASER TECHNOLOGY DEVELOPMENT ROADMAPS

The definition of specific laser technology roadmaps for future laser-based particle accelerators flows naturally from the beam requirements of specific applications, and from the choices of laser-based accelerator technologies that may be used to meet these requirements, i.e., laser wakefield acceleration, bubble regime acceleration, etc. For each specific application and laser-based accelerator technology pair, it is possible to both define and rank a set of viable laser architectures and to outline the laser R&D challenges associated with them.

In this section we will systematically present the possible laser architectures associated with the applications and technology-dependent requirements outlined previously. While these do not represent all possible combinations, they are representative of the breath of possible laser architectures that may be required to meet future accelerator applications.

For each combination of application and accelerator technology choice, representatives of the laser community were asked to

a) Propose specific laser architectures that might meet the accelerator-community-defined laser requirements, with emphasis on those requirements deemed to be of highest importance.
b) Numerically rank, on a scale of 1 to 7, the technical readiness of the each laser architecture to meet each of the specific laser requirements, i.e. pulse energy, pulse repetition rate, wall plug efficiency etc. The readiness scores were: 1 – concept only; 2 – initial modeling has been done; 3 – positive small scale tests have been performed; 4 – numerical scaling has been completed; 5- a scaling demonstration has been completed; 6 – high confidence exists based on previous experiments and modeling; and 7 – an existing system of this architecture has demonstrated an ability to meet the specific requirement
c) Subjectively evaluate (high, medium, or low) the technical difficulty of meeting each of the specific laser requirements with each laser architecture.
d) Provide comments where appropriate regarding technical issues or difficulties each specific architecture has in meeting the requirements.

These laser community evaluations are summarized in Table 5-1.

It should be noted that in the joint task force, the laser requirements provided by the accelerator communities were taken at face value by the laser community, i.e., no feedback was provided regarding what requirements, if eased or adjusted, might open new and possibly more attractive laser architectures for consideration. Suggestions for such changes are included in the summaries that follow.

Even though each application looks for separate parameter requirements, many or all applications for HEP that we examined in this white paper need improvements of technologies on efficiency and average power in particular. This means that we could adopt a strategy of research and development of the following kind. Less technologically demanding applications can be deployed in early stages of research, while we take advantage of these technical breakthroughs and industrial developments along the way to the more demanding applications such as colliders.

5.1. Example: TeV Collider based on a laser plasma accelerator

The summary of requirements put forth by the accelerator community is given in Table 5-1, with a subjective evaluation of the relative importance (from 1: low to 10: critical) of the given requirement relative to the particular application. For example, with respect to the TeV collider application, it is suggested that cost and wall plug efficiency are critical requirements, while the pulse duration and pulse energy are not.

Various combinations of pulse duration and pulse energy can be used to achieve the same net total acceleration per stage. The suggested choice of 56 fs and 32 J at 13 Hz per 10 GeV stage constrains the possible set of laser approaches that may be considered to meet these requirements. In particular the pulse duration requirement constrains the choice of laser gain media to those either directly capable of producing of pulses of 50 fs or requires the further pulse compression of self-phase-modulated pulses of slightly longer duration, e.g., 150 fs.

The laser architecture choices considered are outlined in Table 5-2.

The primary challenges for the laser designer are the removal of heat from the laser gain media while maintaining beam quality and the simultaneous operation of the laser at wall plug efficiencies approaching 50%. The pulse energy and repetition rate requirements imply an average laser power for each 10 GeV acceleration stage of 420 kW.

High quality beams with MW-class average power have been produced by military chemical laser systems; however, this technology is not applicable for the TeV collider application. Chemical lasers are continuous wave and not pulsed devices, and consume chemicals during their operation and are thus not suitable for operation over many days. Furthermore, the pulse energy requirements for laser plasma acceleration imply the use of a "storage" gain medium (one with relatively low gain and high saturation fluence). This consideration rules out the use of gas laser media or direct laser diode illumination.

Solid-state (crystalline and glass) lasers can have the requisite gain and saturation fluence. However, the state of the art for single-aperture, efficient, diffraction-limited, solid-state lasers is currently approximately 10 kW with efficiencies on the order of 20%. The development of solid-state lasers with higher average power and efficiency is a subject of significant interest to industry, the military and the inertial fusion energy community. These lasers are based on a two-step process in which electricity is first used to produce low-beam-quality coherent radiation from arrays of laser diodes, which in turn is used to pump a solid state laser medium and produce high-beam-quality output.

Relative to flashlamp excitation of solid-state laser gain media, diode pumping puts significantly more energy directly into excitation of the upper laser level and thus reduces the thermal loading of the gain media and increases the overall laser efficiency. That said, the electrical to optical output of such systems are typically well below the desired 50% for the TeV collider application. Overall efficiency is the product of the electrical-to-optical efficiency of the laser diodes and the optical-to-optical efficiency of the diode light excitation of the solid state gain medium. In specific low-power experiments, the conversion of electricity to low-quality beams with laser diodes has been reported to approach 80% efficiency. However, efficiency degrades as the power from the diode laser increases; more typically, high-power diode laser arrays perform at electrical-to-optical efficiencies of approximately 60%. Assuming that figure for electrical-to-optical efficiency, a premium must be placed on the *optical*-to-optical efficiency of diode laser pumping if the desired 50% conversion efficiency for a TeV collider is to be achieved.

Table 5-1: Summary of requirements for a 1 TeV collider (in 10-GeV stages) based on the LPA.

Unit cell laser challenges	**Specification**	**Importance (1 low … 10 high)**
pulse energy (J)	32	6
pulse duration (fs)	56	6
effective pulse repetition rate (kHz)	13	8
macrobunch repetition rate	not specified	na
microbunch repetition rate	not specified	na
laser wavelength (microns)	1	5
average power (kW)	420	8
contrast	not specified	na
temporal profile	Gaussian	na
pulse stability %	1	8
laser efficiency (wall plug)	50	10
polarization	100 to 1 linear	6
laser beam quality	<M2=2	7
laser pointing (micro-radian)	1	8
% availability during operation	not specified	na
availability specification	not specified	na
ceo phase stability	not specified	na
timing jitter (fs)	10	8
number of unit cells	50	8
optical transport losses	not specified	na
cost ceiling	<$7B	10

Table 5-2. Laser architecture choices for TeV collider based on the LPA

Application and Technology	Yb:CaF2 Fusion Arch.		Phased Fibers		Mix Nd:Glass w/SPM		Thin Disk Yb:CaF2		Yb:CaF2 Heat Capacity		Diode Pumped Ti:A2O3	
1TeV LPA (10 GeV stages)												
unit cell laser challenges	readiness	difficulty	readiness	difficulty	readiness	difficulty	readiness	difficulty	readiness	difficulty	readiness	difficulty
pulse energy (J)	4	Medium	7	Medium	7	Low	3	Medium	4	Medium	6	Medium
pulse duration (fs)	4	Medium	4	Medium	3	High	4	Medium	4	Medium	7	Low
effective pulse repetition rate (kHz)	4	Low	4	Low	4	Low	4	Low	4	Low	7	Low
macrobunch repetition rate												
microbunch repetition rate												
laser wavelength (microns)	7	Low	7	Low	7	Low	7	Low	7	Low	4	High
average power (kW)	3	High	2	High	3	Medium	3	High	3	High	3	High
contrast												
temporal profile												
pulse stability %	5	Medium	6	Low	5	Medium			5	Medium	5	Medium
laser efficiency (wall plug)	1	High	3	Medium	1	High	1	High	1	High	0	High
polarization												
laser beam quality												
laser pointing (micro-radian)												
% availability during operation												
availability specification												
ceo phase stability												
timing jitter (fs)												
number of unit cells												
optical transport losses												
cost ceiling	7	Low	2	Medium	7	Low	7	low	7	Low	4	Medium

Six possible laser architectures were considered for this application.

a) Diode pumped Yb:CaF2 based on fusion laser architectures.
b) Large phased arrays of single mode fibers.
c) Diode pumped Nd:Glass with self phase modulation.
d) Diode pumped thin disk Yb:CaF2.
e) Diode pumped Yb:CaF2 heat capacity laser.
f) Diode pumped laser pumping Ti:sapphire.

It should be noted first that the pulse duration constraint of 56 fs limits the choice of gain media to either Yb:CaF2, which has both high intrinsic efficiency and sufficient bandwidth to support 56 fs pulses; Ti:sapphire, which has sufficient bandwidth for pulses shorter than 56 fs but low intrinsic efficiency; or Nd:Glass, which has relatively high intrinsic efficiency but does not have the bandwidth to support 56 fs pulses directly. In the latter case it is assumed that one could create ~200 fs pulses and that these pulses could be further reduced in duration via an appropriate self-phase-modulation arrangement.

For the TeV collider application the general consensus is that approach (f) is not viable. It is not conceivable that this approach could produce 50% wall plug efficiency, since the theoretical quantum efficiency for green (532 nm) wavelength pumping of Ti:sapphire is only 56%.

Approaches (a) though (e) all have conceivable paths forward, but in each case, 50% wall plug efficiency is a daunting challenge and well beyond the current state of the art. Of these, (a) and (e) leverage considerable outside investments, from the inertial fusion energy community and laser weapons communities respectively. The principal advantages of these approaches are that they appear to have viable, well-defined costs, which fit within the cost constraints of the TeV application. The development challenge is with respect to increasing the optical-to-optical conversion of the overall system.

Approach (c) is similar but requires an additional step of pulse compression after amplification. This pulse compression step may degrade the overall efficiency of the system and add to system complexity.

Approach (d) leverages the development of high average power lasers for industrial materials processing. The primary issue here will be extraction of high energy pulses from the final amplifiers, specifically the control of amplified spontaneous emission or ASE.

Approach (b) has the highest single-aperture efficiency; in some cases > 30% wall plug efficiency has been demonstrated. However, phasing of beams adds significant complexity and thus a greater challenge with respect to meeting the cost requirement of this application. In this case, if one assumes a single aperture pulse energy that is at the current state of the art, one would need approximately 32,000 fiber apertures per 10 GeV stage. To fit within the cost requirements, each fiber sub-unit must cost less $2000, not including hardware and software required to phase one unit to another. While the telecom industry has demonstrated low unit fiber laser costs, these systems are generally not as complex as those required to produce energetic, short duration pulses, and do not require phasing of single apertures, much less thousands of apertures as is assumed in the TeV accelerator case. Clearly the first R&D step in this case would be the efficient demonstration of tens of apertures to produce a coherent short pulse output. (A detailed discussion of fiber lasers, their R&D challenges, and a roadmap for further development is presented in Section 5.3 below).

5.2. Roadmap for medical laser development

Developing laser systems that are adequate for driving medical plasma accelerators with the required parameters proposed here will likely take another 10-20 years. There are several ongoing and near-term projects addressing these needs at various places in the world. Those must have clear quantitative requirements to fulfill the declared and approved targets. Success with those ongoing projects could correspond to achievements in the specified time windows. Their time structure and the currently envisaged roadmap need to be brought to mutual agreement.

Right now the cost of conventional carbon therapy facilities (in total of the order of 100 M€) allows only a few to be built in any given country. With laser acceleration, a device on a reasonably compact scale–closer to that of photon therapy devices—should be available if future technology developments are achieved.

The complete integrated accelerator system (ILDIAS) consists of not only a laser but also targets (particle sources), beam lines, instrumentation for diagnostics and control, and a sophisticated delivery subsystem. Clearly, these companion technologies must be developed in parallel with laser systems. In particular, an extremely thin but robust film or pneumatic target has to be developed for a carbon system.

For this exercise we used clinical parameters from the Heidelberg HIT facility, but in the future they should be compared with other new clinical facilities in the USA and Asia.

5.3. Fiber laser path to high energy and high power accelerator drivers

In 1985, the University of Southampton rediscovered fiber lasers [1]. Since then developments in low loss rare earth doped optical fiber technology [2, 3] combined with improved reliability, brightness, efficiency and packaging of diode pump lasers [4-6] has quickly led to very-high-power fiber laser systems [7-9]. These systems leverage the waveguide properties of optical fiber in order to achieve exceptional wall plug efficiencies (>30%) and diffraction limited beam quality with high average output powers (>10 kW). Further, these lasers can be manufactured in all-glass monolithic systems in which the light is always contained in fiber core that acts as both waveguide and continuous spatial filter. The result is an efficient, high power laser system that is inherently robust. Once properly packaged, a high power fiber laser system is simple to operate (it is essentially a turn-key system) and requires minimal to no maintenance. These advantages make fiber lasers the first choice for high average power laser applications.

However, Laser Plasma Accelerators as well as nearly all of other laser uses envisioned in this White Paper (with the exception of Direct Laser Acceleration) require short or ultrashort pulses with energies in the range 1 J – 100 J per pulse. This pulse energy range constitutes major technical challenge for fiber lasers, since an individual single-mode fiber laser is limited to pulse energies of tens of mJ at most (ultrashort-pulse fiber CPA is limited to ~1 mJ). *Consequently, the only viable general solution is to combine multiple fiber lasers*.

This section outlines the general path towards achieving required energies with a combined fiber-laser system, reviews the current state of the art in commercial and R&D fiber lasers, outlines the physics issues that need to be addressed to scale output power and pulse energy further, discusses needed component technology developments, and lays out a road map for an R&D path showing how fiber laser technology can meet the laser needs of the accelerator community.

5.3.1. Concept of an Ultrashort-Pulse Fiber CPA Array (Coherent Amplifier Network – CAN)

Generation of high-energy ultrashort pulses in a good quality beam (sufficiently close to the diffraction limit to provide small spot sizes and long focusing depths required for driving laser-plasma interactions) can be achieved through beam combination of a large number of fiber chirped-pulse amplification channels. A generic conceptual schematic of such a system is shown in Figure 5-1. Note that this schematic is not intended to suggest any specific details of implementing such a system, but rather to outline general structure and to identify key components and issues, as well as to evaluate advantages of this approach and its performance potential.

Regardless of any specific technical implementation, a beam-combined ultrashort-pulse fiber laser array in general should consist of the following main parts and components: ultrashort-pulse oscillator, pulse stretcher, fiber amplifier array, beam combining mechanism and associated controls, and pulse compressor. A fiber amplifier array should be a highly integrated, compact and robust structure using a variety of all-fiber components (e.g. pump/signal combiners, fiber star-splitters, etc.) and integrated micro-optical components (e.g., fiber-pigtailed amplitude and phase modulators, optical isolators, etc.). Each individual amplifier channel will consist of 2 to 4 longitudinally-cascaded fiber-amplification stages, with optical gating and optical isolation required between all or some of the stages.

A key advantage of the proposed approach is that it is not subject to thermal loading issues, which constitute the main challenge to any other high-power laser approach. For achieving the required high energies, the total fiber-amplifier channel count will be on the order of 10^4. Therefore achieving ~1 MW of total average power from an array will only require up to ~100 W per individual fiber amplifier channel. Such thermal loading is rather moderate for a fiber amplifier; consequently, thermal management of the whole array is an engineering problem, solvable with already existing means. Indeed, it is reported that incoherently-combined fiber laser systems that achieve 50 kW have been built using over a hundred of individual fiber amplifier channels in a compact and robust package [16]. Other advantages are associated with the anticipated compact size, robustness, reliability and high wall-plug efficiency of a fiber amplifier array.

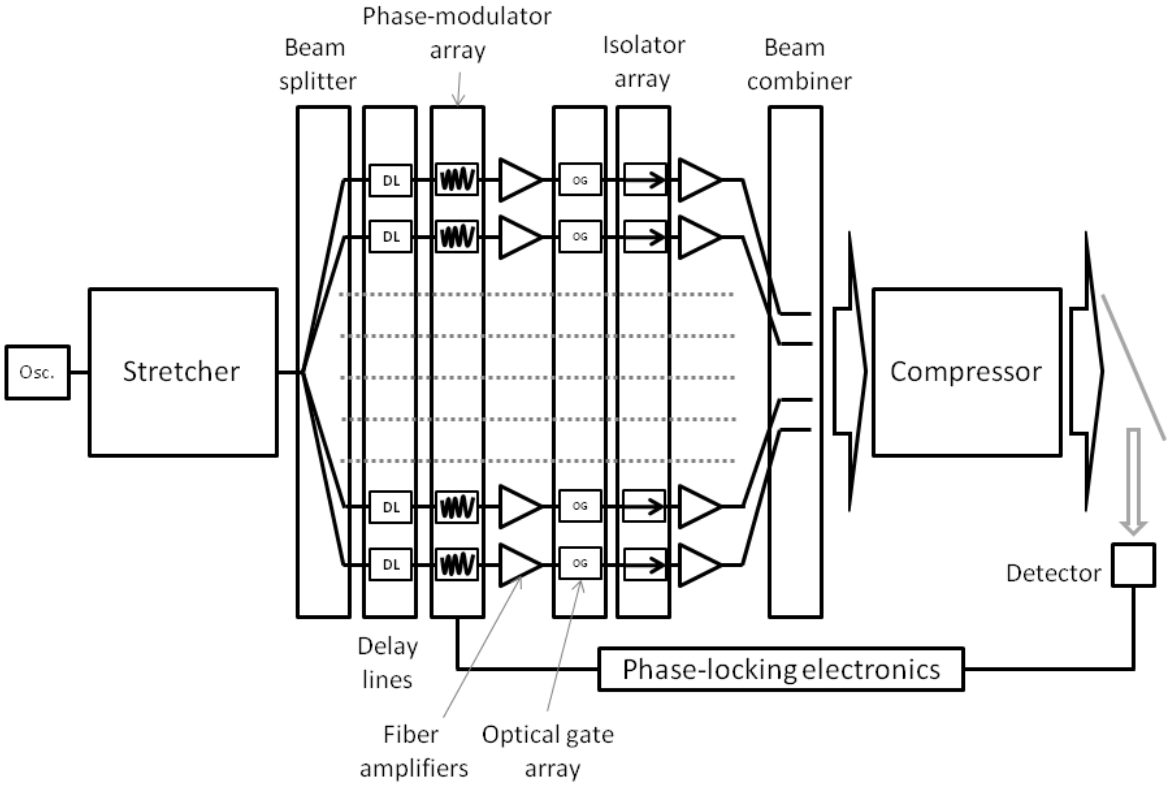

Figure 5-1. A generic beam combined fiber laser will consist of a mode locked master oscillator, followed by a pulse stretcher, a splitter to seed each unit cell individually, components to control/time/adjust pulses in each amplification arm, an amplifier chain, a mechanism to recombine the pulses into a single beam and a compressor. The output will likely include a splitter to pick off part of the beam for analysis, as well as electronic feedback in order to maintain good control of the laser system.

The following general challenges are associated with implementing this coherently-combined fiber-array architecture.

5.3.1.1. First general challenge: Combining the energy from a large number of individual channels into a single beam.

There are a variety of methods for combining the output of fiber lasers. Most of these methods have been focused on combining CW fiber lasers. R&D is needed to develop the most promising of these methods for pulsed fiber laser systems. These methods include but are not limited to:

- Coherent combination via active phase control.
- Spectral beam combination.
- Hybrid systems combining ns class pulses and then employing them as a pump for an OPCPA or bulk laser system.
- Combination via a non-linear effect such as stimulated Raman or Brillouin scattering.

Since a very large number of individual channels will be needed to be combined to provide with the required pulse energies, it is critically important to understand what physical factors that affect the array-size scalability of these various methods; the efficiency of any proposed method; and the way any given method will synthesize a high-fidelity wavefront from the individual fibers' output. The next subsection reviews fiber laser beam combining, including the state of the art and the major physics issues.

5.3.1.2. Second general challenge: Development of "unit cell" shorter pulse fiber lasers with both good pulse quality and CW-class wall-plug efficiency.

The applications envisioned in this document in general require 30-100 fs pulses with good pulse quality and high efficiency. Assuming the beam combination system does not significantly degrade the pulse quality and is efficient in its use of unit cells, then a key to bringing CW fiber lasers to many of these applications is improved unit cells. The issues are discussed in the section below on single-aperture ultrashort pulse fiber laser systems, and can be summarized as follows:

- Improving the amplification bandwidth of fiber lasers.
- Improved dispersion control techniques.
- Understanding and optimizing the trade-offs between efficiency and non-linearities.

5.3.1.3. Third general challenge: Cost and manufacturability involving a large number of individual fiber-laser/amplifier channels.

Since reaching multi-joule pulse energies will require combining of a very large number of individual channels it is critically important to (i) maximize pulse energy per individual channel thus reducing total array size, and (ii) develop fibers and all other required components for the integrated FCPA arrays such that sufficiently low cost per channel could be achieved and practical assembly of such a large-count complex system could be implemented. Note that there is a direct trade-off between maximum pulse energy per individual channel and channel cost: lowering cost per channel allows accommodate lower energies per individual FCPA channel, which would mitigate detrimental effects of fiber nonlinearities on the phase-locking accuracy of a large FCPA array and on the pulse-shape fidelity of the generated ultrashort pulses.

5.3.2. Fiber Laser Combining: state-of-the-art, physics issues and future potential

Beam combining is a general approach of overcoming power or energy limitations of a single laser, and it has been demonstrated with solid-state, fiber and semiconductor lasers. Beam combining of fiber lasers is probably the most promising due to the suitability of fiber-optic technology for compact monolithic integration. Currently, commercial telecom or high-power cw fiber lasers are assembled from standardized fiber-optic components (e.g., pump-signal combiners, gain and passive fibers, and fiber-pigtailed micro-optical components such as optical isolators, modulators, spectral filters, etc.). Assembly is accomplished using standard fiber-splicing techniques in which fiber leads of different components are fusion-spliced together into a monolithic fiber path, thus eliminating any free-space misalignment and

providing a very robust laser system, which in many respects can be described as an optical circuit. Such assembly is also highly compatible with practical manufacturing techniques, with which large numbers of such monolithic fiber lasers can be built in an automated and cost-effective manner.

There are two general approaches of combining laser beams: *incoherent combining*, when the phase differences between individual beams are not fixed, and *coherent combining*, when phase differences between individual beams are fixed.

Incoherent combining can be further subdivided into *spectral combining* and *incoherent power addition*. In spectral combining each individual beam has a different wavelength compared to other beams and the combined beam is formed by spectrally-overlapping these individual beams using spectrally-selective combining elements. These spectral combining elements can be either using spatial dispersion (diffraction gratings [10], volume Bragg gratings [11]) or spatial-dispersion-free approaches (sharp-edge spectral filters [12]). Power scaling potential is primarily determined by the power handling potential of the combining element, but also depends on the maximum number of channels that can be combined with a given element, and on power per laser beam.

It is anticipated that combined powers in the range from 10 to >100 kW will be achievable. Current state of the art, however, has reached powers at the kilowatt level: the best result so far is 750 W with VGB [13], 2 kW with diffraction gratings [14], and 200 W with sharp-edge filters [15]. In incoherent power addition, all individual fiber laser outputs are simply combined in a fused fiber bundle (or spliced onto la arge-core multi-mode fiber), thus providing straightforward overall power increase by sacrificing beam quality. Such sources are currently available commercially with >10 kW of average power [16], and with reported highest powers exceeding 50 kW.

In coherent beam combining, *passive* and *active beam phasing* methods can be distinguished. Active beam phasing methods rely on electronic feedback and on phase modulation devices to control phase of an each individual beam. Passive beam phasing methods rely on optical feedback to "self-lock" all individual laser channels in the array [17]. However, all existing passive phasing methods have a very limited array-size scaling potential. For example, it has been shown that in a self-locked fiber amplifier array combining efficiency becomes less than 80% for array sizes exceeding ten elements [18]. Nevertheless, up to 710 W of average cw power has been demonstrated from a four-element passively combined fiber laser array [19].

Active coherent phasing currently appears to be best for combining large numbers of individual laser channels. In terms of power, the best coherent phasing result demonstrated so far is combination of five individual continuous-wave fiber lasers with the total power of 725 W [20]. Accuracy of coherent phasing in this experiment has been better than $\lambda/60$, which is sufficient for coherently phasing $\sim 10^2$ individual channels [20]. Several methods of converting coherently-phased tiled-fiber array output into a diffraction-limited beam (focusable to a single good-quality near-filled spot) has been explored using diffractive optics [21], multi-mode interference effects in hollow waveguides [22], and different configurations of binary diffraction gratings [23].

5.3.3. Single-aperture (individual-channel) average-power scaling: state-of-the-art, physics issues and future potential

High average power continuous wave (CW) fiber lasers in which the only important parameters are output power, beam quality and wall plug efficiency are commercial products. Systems from IPG

Photonics, Rofin Sinar, Trumpf, JDS Uniphase and numerous others consistently achieve >30% wall plug efficiency and diffraction-limited output powers at 1 μm wavelength in the range of 1 W to 10 kW in reliable, cost-effective and compact packages. Non-diffraction-limited (but still very bright) commercial fiber lasers can achieve even higher powers (>100 kW, limited only by cost) with similar wall-plug efficiencies, maintenance and packaging features. A review of these companies' web sites will quickly bring an interested individual up to speed on current capabilities [24-27].

Single frequency fiber lasers have achieved >600 W output powers in the lab [8] while lasers at 2 μm and 1.5 μm wavelengths have reached output powers of only 885 W [28] and 300 W [29] respectively to date. Wall-plug efficiencies of these systems are also active R&D topics. While commercial 1 μm ytterbium fiber lasers convert diode light to laser light with slope efficiencies of 85%, their thulium (2 μm) and erbium (1.55 μm) cousins have only reached slope efficiencies of 64% [28] and 42% [29] at power levels greater than 100 W. Single-frequency thulium and erbium fiber lasers are also available from commercial vendors, though at lower powers (<500 W at the time of this writing) and lower wall plug efficiencies than achievable in ytterbium fiber lasers. However, the commercial marketplace is rapidly evolving in this area and it is recommended to check the commercial vendor web sites for the most up-to-date information.

Straightforward power scaling of continuous wave fiber lasers has been studied in detail [30]. This study considered all major thermal, nonlinear, damage, and bend limits to power scaling of CW fiber lasers. A key result of this study was that diffraction limited CW Yb^{3+} fiber lasers scaled based upon current optical fiber technology are limited in output power to a maximum of 3 6kW, with practical limits likely in the 10-20 kW range. This upper bound on CW laser power exists because of an interaction between the nonlinear limitation of stimulated Raman scattering and a thermal limitation of a refractive index change in the fiber core due to heating (this shrinks the fiber mode field diameter, which will lead to damage or nonlinear effects). While an optimum core diameter and fiber length are required to reach the maximum output power, no combination of these parameters enables one to exceed this maximum output power, which is set almost entirely by physical constants (see Equation 1):

$$P_{\max} = 4\pi \sqrt{\frac{\eta_{laser} \cdot k \cdot \lambda^2 \cdot \Gamma^2 \cdot \ln(G)}{2 \cdot \eta_{heat} \cdot \frac{dn}{dT} \cdot g_R}} \qquad (1)$$

where h_{laser} is the laser efficiency (85%), k is the thermal conductivity (1.38W/(m-K)), l is the laser wavelength (1.08μm), G is the overlap of the fiber mode field diameter with the fiber core diameter (0.75), G is the gain (10), h_{heat} is the fraction of the energy deposited as heat in the core (0.1), dn/dT is the thermo-optic coefficient (11.8X10^{-6}/K) and g_R is the Raman gain coefficient (0.5X10-11 m/W).

Numbers in parentheses are for Yb^{3+} fused silica fiber lasers. P_{max} for Tm^{3+} and Er^{3+} has been calculated as 36 kW and 54 kW respectively [31]. P_{max} can be calculated for non-silica materials also [31] but these materials are not as advanced in terms of their fabrication and they are not considered further here. It should also be noted that Tm and Er are not as advanced as Yb even in fused silica, and further development of those systems is also needed (but this development is more likely to lead to a fruitful result with a reasonable investment).

Equation 1 was developed for CW fiber lasers; however, it can be extended to pulsed fiber lasers if one modifies the Raman scattering limit equation from the reference to account for the peak power in a pulsed fiber laser, which is related to the average power by the repetition rate W and its pulse width t by

$$P_{avg} = \Omega \cdot \tau \cdot P_{peak} \tag{2}$$

Substituting equation 2 into the power scaling analysis leads to a maximum average power for pulsed fiber lasers that is related to the CW value given in equation 1 by

$$P_{\max}^{pulsed} = \sqrt{\Omega \cdot \tau} \cdot P_{\max} \tag{3}$$

However, there is an additional limit in that pulsed lasers cannot exceed a peak power given by the self-focusing limit [36] (3.7 MW). Assuming (very liberally) that fiber core size can be scaled without penalty, equations 2 and 3 can be plotted for various pulse widths as a function of repetition rate. See Figure 5-2, where the minimum of Equations 2 and 3 has been plotted vs. repetition rate.

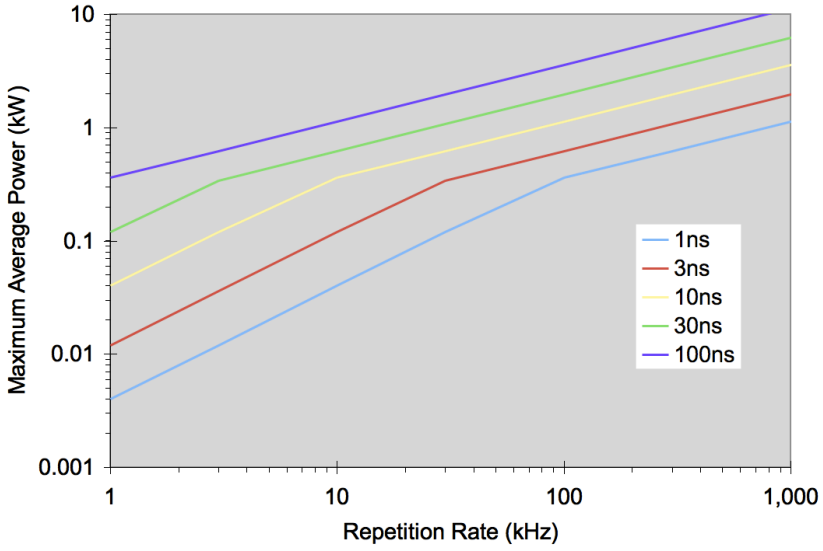

Figure 5-2. Pulsed laser average power vs. repetition rate as a function of pulse width.

In Figure 5-2 a clear kink is observed in allowable average power vs. repetition rate. The allowable output power rises linearly with repetition rate (described by Equation 2) until thermal effects become significant, and the average power then rises as the square root of the repetition rate. The power at which this occurs can be found by setting equations 2 and 3 equal to each other. Doing so, we find the $\sqrt{\Omega\tau}$ = P_{max}/P_{peak}, so the power at which the kink occurs is $P_{\max}^2 / P_{peak}$ or 324W using 36 kW for P_{max} and 4 MW for P_{peak}. Given that at average powers above 324 W, thermal effects limit the results, this in turn will limit pulse energy below that achievable from self-focusing (Figure 5-3).

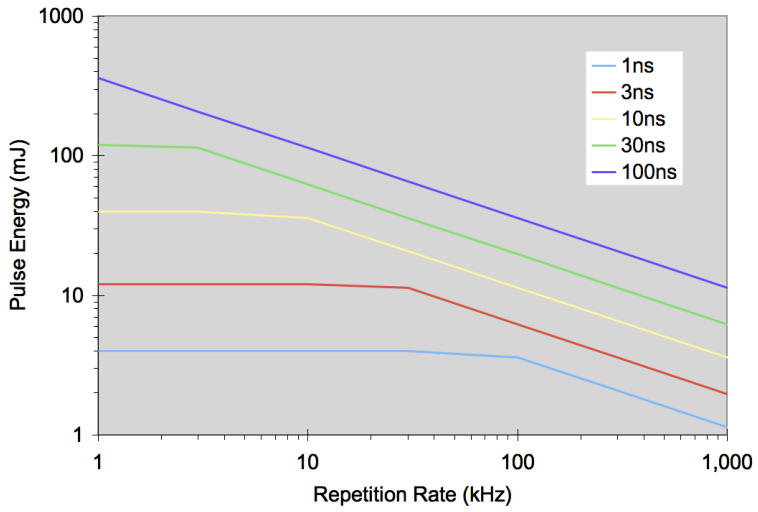

Figure 5-3. Pulse energy limits of a fiber laser as a function of repetition rate and pulse width. The flat regions are self-focusing limited, the sloped regions are thermally limited.

A key point of this section is that scaling the average power of pulsed fiber lasers beyond 324 W while maintaining self-focusing limited peak powers in the fibers is not possible using straightforward aperture scaling. Thus R&D that addresses this issue may help push fiber lasers into new application spaces. Some possible areas of improvement include, but are not limited to, the design of specialty fiber waveguides that minimize thermal lens effects, minimize self-focusing, and suppress stimulated Raman scattering.

5.3.4. Single-aperture pulse-energy scaling: state-of-the-art, physics issues and future potential

Pulse energy limitations of a single aperture fiber laser represent the most stringent constraints. As discussed previously, a single-aperture fiber laser is limited to the millijoule range; consequently, one must resort to beam-combined fiber-array systems as a potential solution to laser-driven accelerator applications. In principle there are three types of pulse-energy constraints in a fiber laser: (i) amplifier saturation when energy extraction exceeds the stored energy, (ii) optical damage, and (iii) nonlinear effects. Constraints (i) and (ii) set the limits for the ultimately achievable pulse energies in a fiber laser or amplifier, and constraint (iii) usually determines pulse energies that can be achieved in practice.

Energy stored in a fiber laser or fiber amplifier is determined by the saturation energy $E_{sat} = h\nu_s A/[(\sigma_{es}+\sigma_{as})\Gamma_s]$, where $h\nu_s$ is signal photon energy, σ_{es} and σ_{as} are emission and absorption cross-sections at the emission wavelengths, A is doped area, and Γ_s is signal-mode overlap with the doped area. Theoretically (see, for example [32]) extractable energy is limited to approximately ten times the saturation energy. In practice, however, energy extraction is limited by strong pulse reshaping at pulse energies exceeding saturation energy, as the pulse's leading edge experiences much higher gain than the trailing edge. Practical rule-of-thumb is that extractable pulse energy $E_{extr.} < 3xE_{sat}$. For example, for Yb-doped fused silica fibers at λ = 1064nm (the most mature fiber gain medium, currently the basis for majority of high-power commercial systems) $E_{sat} \approx 0.46$mJ and $E_{extr.} < 1.4$ mJ, for 30-μm diameter core;

$E_{sat} \approx 1.3$mJ and $E_{extr.} < 3.9$ mJ, for 50-μm diameter core; and $E_{sat} \approx 3.3$mJ and $E_{extr.} < 10$ mJ, for 80-μm diameter core.

Optical damage can be due to (i) surface damage to fiber ends at the core-air interface, (ii) dielectric breakdown in the bulk glass (inside fiber core), or (iii) self-focusing in the fiber core. In practice surface damage can always be avoided using fused-silica end-caps, which allow output beam exiting the core to expand, thus reducing intensity at the glass-air interface to below the surface-damage threshold. Bulk-damage threshold fluence in fused silica has been measured to be ~800J/cm^2 at λ = 1064nm and 6.6-ns pulse duration [33].

Dielectric bulk-damage threshold energy is scalable with the core size – it is proportional to the core area (or, alternatively, to the square of the core diameter). Note that the energy threshold $E_{diel.}$ for bulk dielectric breakdown for nanosecond-duration pulses is proportional to the square-root of the pulse duration τ: $E_{diel} \propto \sqrt{\tau}$ [34].

The self-focusing threshold, however, is independent of the core size and is characterized by the critical self-focusing peak power P_{cr} , which is determined by the nonlinear refractive index n_2 value: $P_{cr} = 1.86\left(\lambda^2/4\pi n n_2\right)$ [35]. For long pulses (>10ns) in fused silica and λ = 1064nm critical power is $P_{cr} \approx 3.7$ MW [36], but for shorter than few-ns pulses electrostriction contribution becomes negligible and critical power increases to $P_{cr} > 5$ MW [37].

Pulse energy limitations due to stored energy and optical damage in Yb-doped fused-silica fibers at 1064 nm wavelength are summarized in Figure 5-4. This figure shows maximum achievable pulse energies limited by optical damage as a function of fiber core diameter, calculated for the three pulse durations of 100 ps, 1 ns and 5 ns. It also shows saturation energy E_s and three-time saturation energy $3xE_s$ as a function of fiber core diameter. It is evident that for pulses longer than ~1 ns and core diameters smaller than 50 μm the limiting factor is stored energy, which confines maximum pulse energies to below ~10 mJ. Note that by increasing core size beyond 50 μm one eventually reaches the self-focusing limit, beyond which pulse energy can only be scaled by increasing pulse duration. Note also that for pulses shorter than ~1 ns, optical damage is always a dominant limiting factor and maximum achievable pulse energies are much less than ~1 mJ.

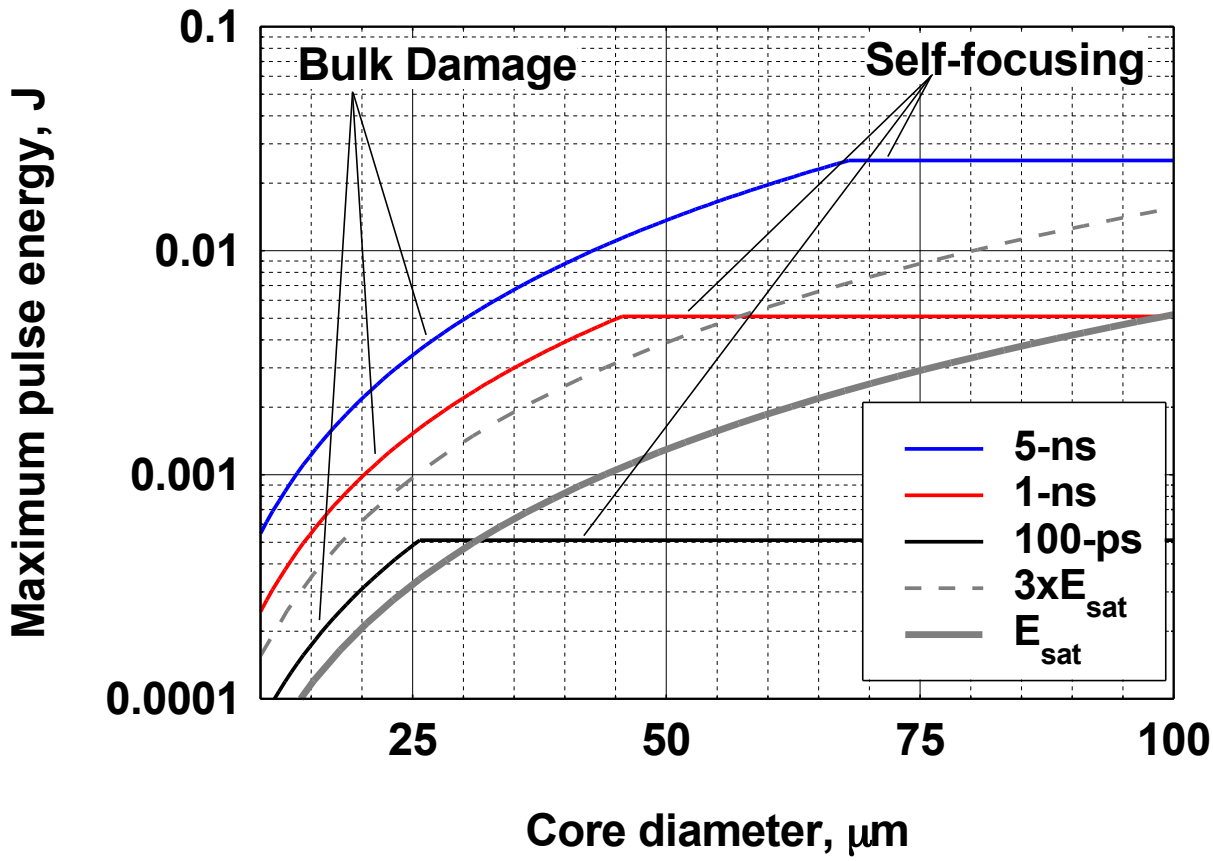

Figure 5-4. Achievable the maximum pulse energies vs. fiber core diameter, as determined by optical damage, self-focusing and stored energy limitations.

In practice, however, limitations due to nonlinear effects are much more stringent. For amplifying long pulses, Stimulated Raman Scattering is usually the limiting effect (see the section on single-aperture power scaling), while for ultrashort pulses self-phase modulation and four-wave-mixing becomes the limiting factor (see the section on singe-aperture ultrashort-pulse fiber laser systems). As a rule of thumb one can always assume that in fiber chirped pulse amplification systems (FCPAs), self-phase modulation imposed limitations are roughly order of magnitude below the ultimate energy limits set by optical damage and gain saturation effects, i.e., single-aperture FCPA systems are limited to ~1 mJ.

Laboratory results to date have demonstrated diffraction-limited, ns pulses of >4mJ [22], albeit with a "fiber-rod" geometry that sacrificed many desirable packaging features. If diffraction limited operation is sacrificed, up to 80 mJ [23] of pulse energy has been extracted from a single aperture in a bendable fiber that retains all the desirable fiber laser packaging features. Up to 6 mJ has been achieved with ~6 ns pulses, with average powers exceeding those from a large (65 μm) core Yb-doped double-clad LMA fiber amplifier with beam quality of M^2 < 1.3 [38]. Bendable diffraction limited fibers are restricted to small apertures of the order of 30 μm. This smaller aperture restricts current state-of-the-art diffraction-limited fiber lasers to output pulse energies of <500 μJ due to extractable energy considerations [24]. In addition to scaling of pulse energy, current pulsed fiber laser R&D is focused on improving pulse quality, particularly temporal contrast and spectral purity.

5.3.5. Single-aperture ultrashort-pulse fiber laser systems: state-of-the-art, physics issues and future potential

Mode-locked fiber lasers have achieved 3 fs pulse durations at 1 μm. Fiber chirped pulse amplifications systems have achieved up to 1 mJ pulse energies at 1 ps pulse widths and 100 μJ pulse energies at <300 fs. However, chirped pulse amplification in fiber lasers is still in its relative infancy and an appropriate investment in R&D could quickly yield significant reductions in pulse width and increases in pulse quality and pulse energy. The following areas are ripe for improvement:

- Increased amplification bandwidth.
- Improved dispersion control.
- Increased pulse energy with good pulse quality and pedestal reduction.
    - High energy pulses in the presence of high B-integral (needed for high efficiency systems).

Bandwidth

Current optical fiber amplifiers at 1 μm (where most work to date has been done) have amplification bandwidths of about 15 nm around 1040 nm. Up to 30 nm bandwidths can be achieved at 1080 nm; however, these amplifiers are inherently longer and thus will have higher B-integrals that can compromise pulse quality. This being said, to date many of the techniques for gain shaping and flattening developed for the telecom industry have not been applied in chirped pulse amplification. Further, a systematic study has not been conducted to discover which fiber amplifiers have the best potential of achieving high pulse energies with broad bandwidths. Instead, attention has focused almost exclusively on Yb^{3+} fiber amplifiers, as Yb^{3+} fibers are most easily obtainable. Exploration of gain flattening, other gain dopants (Nd^{3+}, Pr^{3+}, Er^{3+} and Tm^{3+}) and possibly mixing of gain dopants could prove fruitful for increasing gain bandwidth significantly, and might also improve fiber CPA results at high energy from 300 fs to the 30 fs achievable in fiber mode-locked oscillators.

Dispersion Control

In most CPA systems the amount of material is minimized in order to minimize the impact of material dispersion on the overall dispersion balance of the system. However, in fiber laser systems this approach is simply not possible, and any fiber CPA will need to accept and be able to deal with meters of fused silica in the amplifier chain. While the group delay dispersion (GDD) is relatively easily compensated, higher-order terms can be quite problematic. For example, the third-order dispersion (TOD) term in fused silica at 1 μm has the same sign as the GDD, whereas in a typical grating based stretcher and compressor these terms are opposite in sign. Further, the TOD in an optical fiber is quite small compared to the GDD and thus leads to significant mismatches in the final dispersion balance. This being said, there are a number of promising techniques for dealing with these issues: "grisms" [39], stretcher/compressor mismatches, custom chirped fiber Bragg gratings or chirped volume Bragg gratings, pulse shaping to enable the B-integral to balance the dispersive terms [40], etc. R&D in support of developing a simple to implement dispersion control scheme applicable to high-energy fiber laser systems and robust against pulse fluctuations would be extremely valuable. To do this accurately, the resulting pulses would need to be well characterized.

Efficiency and High Energy Pulses

In any laser system, efficient conversion of pump photons to signal photons necessitates high intensities. In bulk optic laser systems, one achieves high intensities via a tight focus in the gain medium. However, in free space, this leads to a short Rayleigh range and thus a short interaction length. and correspondingly significant heat build-up in a small volume, which is very problematic. Fiber laser systems more easily achieve high powers with high efficiencies because the fiber waveguide breaks the relationship between spot size and propagation length. In other words, high intensity (and thus high efficiency) can be maintained over a length much, much longer than the bulk optic Rayleigh range (enabling easy heat extraction).

However, small apertures required for high intensity (and thus high efficiency) limit pulse energy. Physical limits that demand larger apertures in order to achieve high pulse energy include extractable energy and optical damage. Other physical limits such as stimulated Raman scattering and self-phase modulation (a.k.a. B-integral) depend both on aperture size and on length (thus a shorter length can compensate for a smaller aperture area to an extent). In the end, however, high-pulse-energy lasers and particularly fiber lasers typically attempt to achieve a balance between smaller aperture areas to maximize efficiency and larger aperture areas to maximize pulse energy. In an optical fiber laser this trade-off is often between efficiency and the accumulation of B-integral.

Thus R&D towards short pulse CPA fiber lasers, in which good pulse compression is achieved in the presence of the highest possible B-integrals, is needed in order to achieve the goal of high energy, high efficiency, short pulse fiber laser unit cells. Fiber CPA systems with pulses in the 100 μJ to 1 mJ class demonstrated to date fall into two categories: moderate to high quality pulses generated in fiber lasers systems where the accumulated B-integral for the stretched pulse was less than 2; and lower quality pulses with significant pedestal where the accumulated B-integral for the stretched pulses is greater than 2. However, in order to achieve high system efficiency, in stretched pulses consistent with reasonable sized compressors (2-5 ns), it may be desirable to operate at B-integrals as high as 30. In systems with this degree of self-phase modulation there many effects that can degrade pulse quality and lead to significant pulse pedestals. To this end, R&D that investigates high-energy fiber CPA in the presence of high B-integral would help to open a range of parameter space that contains efficient solutions to many of the currently targeted applications in laser-based acceleration. The alternative is investigation of fiber laser systems in which the efficiency is comparable to a CW laser, but in which the B-integral is <5.

As a final note on efficiency, we note that for repetition rates >10-20 kHz, a pulsed fiber laser and a CW fiber laser can at least theoretically hope to achieve the same efficiency. This is because the pulse repetition rate is much faster than the upper state lifetime of the rare-earth ions in the glass, so little to no power is lost to ASE between pulses. However, as the repetition rate drops progressively below 10 kHz, ASE losses begin to take their toll and the system efficiency drops. This is true of any solid state laser system and will have a negative impact on system design and/or efficiency for operation below 10 kHz.

5.3.6. Components for integration of high power fiber lasers: current status and required future developments

Since envisioned coherently-combined fiber laser arrays would be complex multi-component systems, it is imperative that they would exploit the key advantage of fiber technology: its ability to integrate complete system form all-fiber or fiber-pigtailed micro-optical components. This would ensure (i)

robustness and reliability of the system, which in principle would be turn-key and maintenance-free (in the sense that no optical re-alignment would ever be needed), (ii) compact size, and (iii) cost-effective manufacturability.

This would be similar to the existing commercial multi-kW continuous-wave fiber laser systems, which all are optically-integrated optical systems. However, these existing continuous-wave fiber laser systems are based on relatively small-core (typically <25 μm core diameter) fibers. Ultrashort pulse and high-energy FCPA-array systems envisioned here would require much-larger-core fibers, in order to be able to extract maximally available pulse energies per individual FCPA channel, which, as it has been pointed out at the beginning, is necessary to minimize FCPA-array size and, consequently, the cost and complexity of the system.

The critically important requirements here are that these large-core fibers would be (i) producing single-transverse-mode output, which is critical in order to maintain ultrashort-pulse fidelity; and (ii) would be compatible with conventional fiber fusion-splicing techniques, which is critical for assembling large number of laser channels in an integrated fashion. This means that some of the techniques currently popular for high-energy ultrashort-pulse CPA systems, such as photonic-crystal rods [41]\ (which are not suitable for fusion-splicing integration) or large-core (larger than ~30 μm core) LMA fibers [38] (which would not provide with sufficiently robust single-mode output) would not be suitable for the envisioned FCPA-array solution. At the moment there are possible fiber solutions emerging [42], [43], and some of them are even in the process of commercialization [44], but extensive further work is required to develop these fibers, as well as to develop a complete fiber-optic component technological platform (e.g., all-fiber pump combiners, pigtailed isolators, etc.) for these fibers.

Furthermore, novel fiber-pigtailed components need to be developed in order to meet the requirement for low cost per channel. The issue here is that the envisioned FCPA array should have on the order of 10^4 individual FCPA channels. If the total cost of one module (suitable, for example, for driving a ~1GeV – 10 GeV accelerator cell) should be on the order of ~$10M, then cost per channel should be limited to ~$1000. Current state-of-the-art commercial FCPA systems cost approximately 100× that.

The issue here is not the cost of the fiber or pump diodes per each channel, which, when fiber and diodes are mass-produced, would very likely be reduced to much below $1000 per channel. The issue is the cost of other components, such as phase modulators (used for phasing the individual channels), amplitude modulators (used as optical gates between cascaded fiber-amplifier stages), and even fiber-pigtailed isolators. Cost of these components is likely to remain significantly above $1000 per channel even if mass-produced. The required engineering solution would be to develop array-type elements, which could be then integrated with a complete array, rather than individual FPCA channels. In this case even relatively large cost per element could be acceptable, since cost per channel would remain low.

5.3.7. Pulse Compression Diffraction Gratings

The list of critical-path technologies needed for the next generation of CPA lasers includes advanced pulse-compression diffraction gratings. Compressor gratings must satisfy several requirements, including high diffraction efficiency, high wavefront quality, and high laser damage threshold. Currently available gratings do not possess the combination of laser damage threshold and wavefront quality needed to provide a tightly focused megajoule-class laser. As a result, the irradiance available for laser accelerators

has ample room for improvement. Continual improvement of the following innovations promises to make this possible over the next decade.

A conventional multi-layer dielectric (MLD) grating is composed of a binary surface relief formed in the top layer of an MLD stack[45]. The typical stack (Figure 5-5) consists of a few dozen alternating high- and low-refractive-index layers. By varying the groove height and duty cycle (ratio of pillar width to groove spacing), the diffraction efficiency and electric field intensity are optimized for each application. A taller and thinner pillar shifts the edge of the pillar away from the region of maximum irradiance, thus potentially raising the laser-induced damage threshold of the grating. However, its threshold is strongly influenced by the MLD coating, the ion-etching process used to form the grating pillars, and the final multi-step cleaning process. The presence of contaminants from the patterning and etching processes, found along the pillars of the finished grating, can lead to significant degradation of the laser-damage threshold. Significant progress has taken place as these manufacturing related issues are being actively studied at several research facilities around the world.

The continuous-enfolded grating (CEG) is an alternative grating scheme which avoids the challenges of fabricating narrow binary pillars and takes advantage of the breakthroughs obtained in high power laser mirror technology. This grating configuration involves depositing an MLD coating over a continuous grating, resulting in a corrugated structure in each layer of the multilayer coating. All layers, instead of only the top surface, then act as diffractive structures. There are two benefits to this type of diffraction grating. Etching the top surface of the final component is no longer necessary, reducing a major source of contamination that can affect the laser damage resistance of the completed grating. Also, tall and narrow binary pillars, which are mechanically fragile, are replaced with a relatively flat grating surface.

SEM imaging indicates that current evaporation processes maintain a structured surface for as many as 12 layers, which is a sufficient number to achieve high diffraction efficiency[46]. Manipulation of the surface mobility of the deposited coating, incidence angles, coating materials, deposition method, and design types are being explored to maintain the desired structure following multiple layers of the coating. Both approaches allow the possibility of metal-dielectric hybrid designs for high bandwidth, short pulse applications. A reduction in the total number of layers reduces the total stress, and thus the wavefront error, accumulated in the coating, thereby increasing the focal spot irradiance. The results from preliminary investigations of the CEG motivate further development aimed at scaling this technology towards meter-size high-power gratings.

For applications in high-flux laser acceleration, compressor gratings must withstand the challenges imposed by heat generated from high average power illumination. A coating's design and manufacturing process, as used to fabricate large diffraction gratings (whether all dielectric or metal-dielectric hybrid), plays an important role in determining the power handling capability. Energetic ion or electron bombardment of the growing film can modify its structure and final stress. Plasma-assisted deposition has been shown to significantly increase the coating performance for 1053-nm applications at both 1 ns and 10 ps, while balancing the overall film stress to achieve high wavefront quality. Ion-beam sputtering has been used to fabricate ultralow-loss coatings with demonstrated damage thresholds at 1 to 10 ps.

The primary benefits of these coatings are their high density, their insensitivity to changes in humidity, and their greatly reduced defect density, all desirable for high average power applications. In addition, light-weighted substrates, equipped with proper cooling channels, could potentially be applied to diffraction gratings to achieve high wavefront quality under the stress associated with high average power

conditions. Furthermore, the adaptive optics technology, previously developed for mirrors, is currently being considered for the wavefront control of large diffraction gratings.

The energy-limiting component is the final grating in a compressor, which is the most susceptible to damage because it experiences the shortest pulse and therefore the highest peak intensity. The ultimate limitation for damage threshold of optical materials forces the laser community to seek configurations which increase the total area of the grating compressor. For this reason, the size of individual gratings has reached one meter. Grating tiling has been pioneered at LLE to coherently combine multiple gratings to form a larger grating*[47]*. However, even in the case of meter-size gratings, the coherent combination of grating arrays provides a means to increase further the energy of CPA lasers. Modern electronic technology, such as capacitive sensors and piezoelectric actuators, supports positioning and control at the nanometer level. The tiling of meter-size gratings can significantly benefit from ongoing advancements in mirror-array technology that are presently being demonstrated with space telescopes that exceed 30 square meters in area (Figure 5-6). In combination, continued advancement of these technologies provides a path towards higher energy, and higher brightness, CPA lasers.

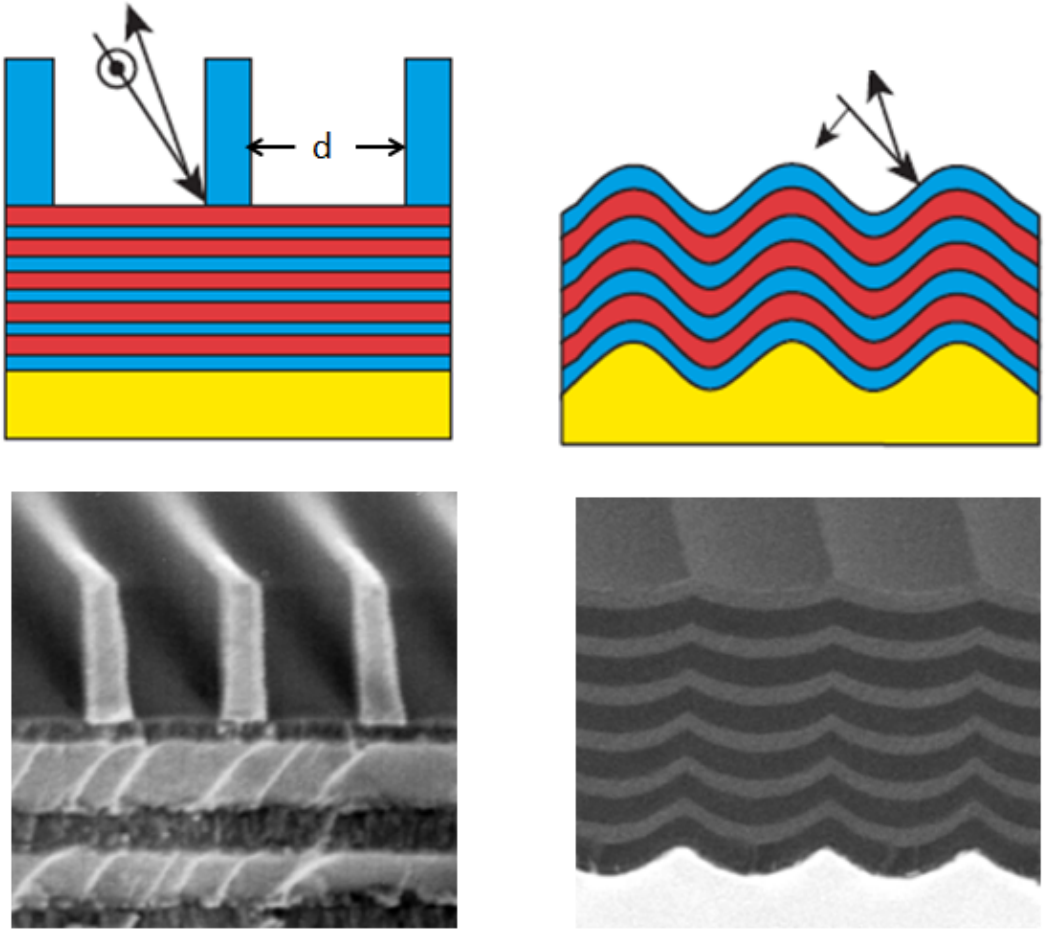

Figure 5-5. Binary MLD gratings have been developed over the last decade to realize the high energy petawatt laser (left graphic and SEM image). The continuous enfolded grating provides key advantages similar to mirrors that exhibit high laser damage threshold (right graphic and SEM image). The dispersions required for compressor gratings correspond to spacing d, which is between 400 to 600 nm.

Figure 5-6. Coherently combined grating arrays provide a means to scale the energy of CPA lasers (upper). The tiling of meter-scale gratings will build on advancements in mirror-array technology that have been demonstrated with space telescopes now approaching 30 square meters in area (lower).

5.3.9. Fiber Laser Roadmap

1. Investigation and development of beam combining techniques suitable for combining >1000 ultrashort pulse fiber unit cells
    a. Physics of coherent FCPA arrays
        i. Array architecture compatible with 10^4 element coherent phasing
            1. Channel-locking/identification schemes
            2. Accuracy of phase-locking
        ii. Array-size scalability
        iii. Effects of nonlinearities (at max pulse energies) on the coherent combining
        iv. Diffractive-optics reshaping of tiled coherently-phased beams
    b. Spectral combining of FCPA arrays
    c. Hybrid systems with fiber laser based nanosecond beam combined pump lasers
        i. Ti:Sapphire (efficiency?)

ii. Fiber pumped OPCPA
   d. Beam combining based upon stimulated Raman or Brillouin scattering
2. Development of efficient, high energy, 40fs unit cells with high pulse contrast
   a. Efficient 100nm bandwidth fiber amplifiers
   b. Tools for balancing the dispersion of a fiber laser system over > 100nm bandwidth
   c. Tools for dealing with the large B-integrals and mitigating the influence of these effects on pulse quality OR efficient low B-integral unit cells
   d. Tools for minimizing other detrimental non-linear effects
3. Components
   a. Large-core fibers and fiber components for monolithic large-core integration
   b. Phase-modulator arrays
   c. Amplitude-modulator (optical gate) arrays
   d. Fiber-pigtailed optical isolator arrays
4. Engineering/development of 1MW average power pulse compressors

5.3.10. Fiber-Laser References

1. R.J. Mears, L. Reekie, I.M. Jauncey and D.N. Payne, "Low noise erbium doped fiber amplifier operating at 1.54μm," Electronics Letters, vol. 23, pp. 1026-1027 (1987).
2. B.J. Ainslie, S.P. Craig and S.T. Davey, "The absorption and fluorescence spectra of rare earth ions in silica based monomode fiber," Journal of Lightwave Technology, vol. 6, pp. 287-293 (1988).
3. H.M. Pask, R.J. Carman, D.C. Hanna, A.C. Tropper, C.J. Mackechnie, P.R. Barber and J.M. Dawes, "Ytterbium-doped silica fiber lasers: versatile sources for the 1-1.2μm region," IEEE Journal of Selected Topics in Quantum Electronics, vol. 1, pp. 2-13 (1995).
4. S.L. Yellen, A.H. shepard, R.J. Dalby, J.A. Baumann, H.B. Serreze, T.S. Guido, R. Soltz, K.J. Bystrom, C.M. Harding and R.G. Waters, "Reliability of GaAs-based semiconductor diode lasers: 0.6-1.1μm," IEEE Journal of Quantum Electronics, vol. 29, pp. 2058-2067 (1993).
5. P. Leisher, M. Reynolds, A. Brown, K. Kennedy, L. Bao, J. Wang, M. Grimshaw, M. DeVito, S. Karlsen, J. Small, C. Ebert, R. Martinsen and J. Haden, "Reliability of high power diode laser systems based on single emitters," Proceedings of the SPIE, vol. 7918, pp. 791802-1-7 (2011).
6. T. Koenning, K. Alegria, Z. Wang, A. Segref, D. Stapleton, W. Fassbender, M. Flament, K. Rotter, A. Noeske and J. Biesenbach, "Macro-channel cooled, high power, fiber coupled diode lasers exceeding 1.2kW of output power," Proceedings of the SPIE, vol. 7918, pp. 79180E-1-8 (2011).
7. V. Gapontsev, V. Fomin and A. Yusim, "Recent progress in scaling of high-power fiber lasers at IPG Photonics," 22nd Solid State and Diode Laser Technology Review Technical Digest, 29 June-2 July 2009, pp. 142 (2009).
8. G.D. Goodno, L.D. Book and J.E. Rothenberg, "Low-phase-noise, single-frequency, single-mode 608W thulium fiber amplifier," Optics Letters, vol. 34, no. 8, pp 1204-1206 (2009).
9. D.J. Richardson, J. Nilsson and W.A. Clarkson, "High power fiber lasers: current status and future perspectives [Invited]," Journal of the Optical Society of America B, vol. 27, no. 11, pp B63-B92 (2010).
10. S. J. Augst, A. K. Goyal, R. L. Aggarwal, T. Y. Fan, and A. Sanchez, "Wavelength beam combining of ytterbium fiber lasers," Opt. Lett. **28**, 331-333 (2003); http://www.opticsinfobase.org.proxy.lib.umich.edu/ol/abstract.cfm?URI=ol-28-5-331

11. Igor V. Ciapurin, Leonid B. Glebov, Larissa N. Glebova, Vadim I. Smirnov, and Eugeniu V. Rotari, "Incoherent combining of 100-W Yb-fiber laser beams by PTR Bragg grating," Proc. SPIE, Vol. 4974, 209 (2003).
12. K. Regelskis, K. Hou, G. Raciukaitis, and A. Galvanauskas, "Spatial-Dispersion-Free Spectral Beam Combining of High Power Pulsed Yb-Doped Fiber Lasers," in Conference on Lasers and Electro-Optics/Quantum Electronics and Laser Science Conference and Photonic Applications Systems Technologies, OSA Technical Digest (CD) (Optical Society of America, 2008), paper CMA4.
13. Armen Sevian, Oleksiy Andrusyak, Igor Ciapurin, Vadim Smirnov, George Venus, and Leonid Glebov, "Efficient power scaling of laser radiation by spectral beam combining," Opt. Lett. **33**, 384-386 (2008); http://www.opticsinfobase.org/abstract.cfm?URI=ol-33-4-384
14. C. Wirth, O. Schmidt, I. Tsybin, T. Schreiber, T. Peschel, F. Brückner, T. Clausnitzer, J. Limpert, R. Eberhardt, A. Tünnermann, M. Gowin, E. ten Have, K. Ludewigt, and M. Jung, "2 kW incoherent beam combining of four narrow-linewidth photonic crystal fiber amplifiers," Opt. Express **17**, 1178-1183 (2009); http://www.opticsinfobase.org.proxy.lib.umich.edu/abstract.cfm?URI=oe-17-3-1178
15. O. Schmidt, C. Wirth, D. Nodop, J. Limpert, T. Schreiber, T. Peschel, R. Eberhardt, and A. Tünnermann, "Spectral beam combination of fiber amplified ns-pulses by means of interference filters," Opt. Express **17**, 22974-22982 (2009); http://www.opticsinfobase.org.proxy.lib.umich.edu/abstract.cfm?URI=oe-17-25-22974
16. http://www.ipgphotonics.com/Collateral/Documents/English-US/HP_Brochure.pdf
17. V. A. Kozlov, J. Hernández-Cordero, and T. F. Morse, "All-fiber coherent beam combining of fiber lasers," Opt. Lett. **24**, 1814-1816 (1999); http://www.opticsinfobase.org.proxy.lib.umich.edu/ol/abstract.cfm?URI=ol-24-24-1814
18. Wei-zung Chang, Tsai-wei Wu, Herbert G. Winful and Almantas Galvanauskas, "Array size scalability of passively coherently phased fiber laser arrays," Optics Express **18**, 9634 – 9642 (2010).
19. T. H. Loftus, A. M. Thomas, M. Norsen, J. Minelly, P. Jones, E. Honea, S. A. Shakir, S. Hendow, W. Culver, B. Nelson, and M. Fitelson, "Four-Channel, High Power, Passively Phase Locked Fiber Array," in *Advanced Solid-State Photonics*, OSA Technical Digest Series (CD) (Optical Society of America, 2008), paper WA4. http://www.opticsinfobase.org.proxy.lib.umich.edu/abstract.cfm?URI=ASSP-2008-WA4
20. T. M. Shay, J. T. Baker, A. D. Sancheza, C. A. Robin, C. L. Vergien, A. Flores, C. Zerinque, D. Gallant, C. A. Lu, B. Pulford, T. J. Bronder, and A. Lucero, "Phasing of High Power Fiber Amplifier Arrays," in Advanced Solid-State Photonics, OSA Technical Digest Series (CD) (Optical Society of America, 2010), paper AMA1; http://www.opticsinfobase.org.proxy.lib.umich.edu/abstract.cfm?URI=ASSP-2010-AMA1
21. Eric C. Cheung, James G. Ho, Gregory D. Goodno, Robert R. Rice, Josh Rothenberg, Peter Thielen, Mark Weber, and Michael Wickham, "Diffractive-optics-based beam combination of a phase-locked fiber laser array," Opt. Lett. **33**, 354-356 (2008); http://www.opticsinfobase.org.proxy.lib.umich.edu/abstract.cfm?URI=ol-33-4-354
22. Radoslaw Uberna, Andrew Bratcher, Thomas G. Alley, Anthony D. Sanchez, Angel S. Flores, and Benjamin Pulford, "Coherent combination of high power fiber amplifiers in a two-dimensional re-imaging waveguide," Opt. Express **18**, 13547-13553 (2010); http://www.opticsinfobase.org.proxy.lib.umich.edu/abstract.cfm?URI=oe-18-13-13547
23. Aimin Yan, Liren Liu, Enwen Dai, Jianfeng Sun, and Yu Zhou, "Simultaneous beam combination and aperture filling of coherent laser arrays by conjugate Dammann gratings," Opt. Lett. **35**, 1251-

1253 (2010);
http://www.opticsinfobase.org.proxy.lib.umich.edu/abstract.cfm?URI=ol-35-8-1251
24. http://www.ipgphotonics.com/
25. http://www.rofin.com/
26. http://www.us.trumpf.com/
27. http://www.jdsu.com/en-us/Pages/Home.aspx
28. P.F. Moulton, G.A. Rines, E.V. Slobodtchikov, K.F. Wall, G. Frith, B. Sampson, A.L.G. Carter, "Tm-doped fiber lasers: fundamentals and power scaling," IEEE Journal of Selected Topics in Quantum Electronics, vol 15, pp. 85-92 (2009).
29. Y. Jeong, S. Yoo, C.A. Codemard, J. Nilsson, J.K. Sahu, D.N. Payne, R. Horley, P.W. Turner, L. Hickey, A. Harker, M. Lovelady, A. Piper, "Erbium:ytterbium codoped large-core fiber laser with 297 W continuous wave output power," IEEE Journal of Selected Topics in Quantum Electronics, vol. 13, pp. 573-579 (2007).
30. J.W. Dawson, M.J. Messerly, R.J. Beach, M.Y. Shverdin, E.A. Stappaerts, A.K. Sridharan, P.H. Pax, J.E. Heebner, C.W. Siders, C.P.J. Barty, "Analysis of the scalability of diffraction-limited fiber lasers and amplifiers to high average power," Optics Express, vol. 16, no. 17, pp. 13240-13266 (2008).
31. J.W. Dawson, M.J. Messerly, J.E. Heebner, P.H. Pax, A.K. Sridharan, A.L. Bullington, R.J. Beach, C.W. Siders, C.P.J. Barty, M. Dubinskii, "Power scaling analysis of fiber lasers and amplifiers based on non-silica materials," Proceedings of the SPIE, vol. 7876, pp. 787611-1-12 (2010).
32. Cyril C. Renaud, et al, "Characteristics of Q-Switched Cladding-Pumped Ytterbium-Doped Fiber Lasers with Different High-Energy Fiber Designs," IEEE JQE **37**, 199 – 206 (2001).
33. W. Torruellas, Y. Chen, B. McIntosh, J. Farroni, K. Tankala, S. Webster, D. Hagan, M. J. Soileau, M. Messerly, and J. Dawson, "High peak power Ytterbium doped fiber amplifiers," Proc. SPIE, vol. 6102, pp. 61020-1– 61020-7, 2006.
34. B. C. Stuart, M. D. Feit, S. Herman, A. M. Rubenchik, B. W. Shore, and M. D. Perry, "Optical ablation by high-power short-pulse lasers", J. Opt. Soc. Am. B 13, 459 – 468 (1996).
35. G. Fibich and A. L. Gaeta, "Critical power for self-focusing in bulk media and in hollow waveguides", Opt. Lett. 25, 335 – 337 (2000)/
also: R. L. Farrow, D. A. V. Kliner, G. R. Hadley, and A. V. Smith, "Peak-power limits on fiber amplifiers imposed by self-focusing," Opt. Lett. 31, 3423-3425 (2006).
36. G. P. Agrawal, Nonlinear Fiber Optics, Academic Press, San Diego, CA (1995).
37. A. Melloni, M. Frasca, A. Garavaglia, A. Tonini, and M. Martinelli, "Direct measurement of electrostriction in optical fibers", Opt. Lett. 23, 691 – 693 (1998).
also: D. Milam, "Review and assessment of measured values of the nonlinear refractive-index coefficient of fused silica", Applied Optics, vol. 37, pp. 546 - 550 (1998).
38. Almantas Galvanauskas, Ming-Yuan Cheng, Kai-Chung Hou, and Kai-Hsiu Liao, "High Peak Power Pulse Amplification in Large-Core Yb-Doped Fiber Amplifiers", IEEE JSTQE, Vol. 13, No. 3, 559 (2007).
39. S. Kane and J. Squier, "Grating compensation of third-order material dispersion in the normal dispersion regime: sub-100-fs chirped pulse amplification using a fiber stretcher and grating compressor pair," IEEE Journal of Quantum Electronics, vol. 31, pp. 2052-2057 (1995).
40. L. Shah, Z. Liu, I. Hartl, G. Imeshev, G. Cho and M. Fermann, "High energy femtosecond Yb cubicon fiber amplifier," Optics Express, vol. 13 pp. 4717-4722 (2005).
41. Fabio Di Teodoro, Michael K. Hemmat, Joseph Morais, and Eric C. Cheung "High peak power operation of a 100μm-core, Yb-doped rod-type photonic crystal fiber amplifier," Fiber Lasers VII: Technology, Systems, and Applications, Proc. of SPIE Vol. 7580, 758006.
L. Dong, J. Li, and X. Peng, " Bend-resistant fundamental mode operation in ytterbium-doped leakage channel fibers with effective areas up to 3160 μm2," Opt. Express 14, 11512-11519 (2006).
42. Chi-Hung Liu, Guoqing Chang, Natasha Litchinitser, Doug Guertin, Nick Jabobson, Kanishka Tankala, and Almantas Galvanauskas, "Effectively Single-Mode Chirally-Coupled Core Fiber",

Advanced Solid State Photonics 2007, Paper ME2, January 28 - 31, 2007, Vancouver, British Columbia.
43. Michelle L. Stock; Chi-Hung Liu; Andrey Kuznetsov; Gaston Tudury; Almantas Galvanauskas; Thomas Sosnowski," Polarized, 100 kW peak power, high brightness nanosecond lasers based on 3C optical fiber", SPIE Proceedings Vol. 7914, Fiber Lasers VIII: Technology, Systems, and Applications, Jay W. Dawson, Editors, 79140U.
44. "Design of high-efficiency dielectric reflection gratings," B. Shore et al., JOSA, May 1997.
45. Private communication (T. Kessler, Laboratory for Laser Energetics).
46. "Demonstration of coherent addition of multiple gratings for high-energy chirped-pulse-amplified lasers," T. Kessler et al., Optics Letters, March 15, 2004.
47. ITT Space Systems Division (formerly Kodak), Rochester, New York.

6. SUMMARY

6.1. Collider work package

The largest challenge for laser technology is a laser-plasma e-e collider up to the 10 TeV goal. The consensus in the world high energy physics community is that the next large collider after the LHC would be a TeV-scale lepton collider. Options currently under study include the ILC (0.5-1 TeV), CLIC (up to 3 TeV) and a muon collider (up to 4 TeV), all using RF technology. The very high gradients (~10 GeV/m) possible with laser plasma acceleration, on the other hand, open up new avenues to reach even higher energy and more compact machines (see W. Leemans and E. Esarey, Physics Today **62**, 44-49 (2009)). This workshop investigated the beam and laser parameters of a 1-10 TeV, 10^{36} $cm^{-2}s^{-1}$ e+e- collider based on two different technologies – laser plasma acceleration (LPA) and direct laser acceleration (DLA). The main challenges to the practical achievement of laser acceleration are: high average power (~100 MW), high repetition rate (kHz to MHz), high efficiency (~40-60%) and a cost that ideally would be an order of magnitude lower than that of RF based technology. The workshop also studied the laser requirements for a 200 GeV $\gamma\gamma$ collider, proposed as the first stage of a full scale ILC or CLIC. The required laser systems for such a collider may be within reach of today's technology.

6.2. Light Source work package

Lasers already play a significant role in existing light source facilities, but face new challenges with future light sources that aim at much higher repetition frequency. Ultrafast (femtosecond) lasers reaching 1-10 kW levels will be required for seeding and user driven experiments. Lasers producing a few joules in 30-50 fs pulses at high repetition rate (100-1000 Hz) could be used to drive laser plasma accelerator. Thanks to their ability to produce GeV-class, ultra-short, high peak current electron bunches, these laser plasma accelerators could in turn drive compact free electron lasers operating in the soft x-ray regime. Higher energy per pulse lasers (~40 J) would be needed to drive multi-GeV electron bunches for hard-x-ray FELs.

6.3. Medical Application work package

The third area of application has been medical applications of laser acceleration of protons/ions and its potential to replace current technology used in tumor therapy. Such lasers are typically very high peak power (PW-class) and require special pulse shapes with very high temporal contrast. Again, multi-kW compact lasers will be needed.

6.4. Laser work package

Laser requirements for the applications discussed above are often many orders of magnitude beyond the capabilities of the lasers used in today's scientific demonstrations, i.e., megawatts versus tens of watts. Laser science representatives at the meeting discussed and outlined how, with appropriate R&D, emerging 100-kW-class industrial lasers, 10-MW-class laser fusion energy technologies and MW-class defense laser systems might be adapted to meet these challenging requirements. Approaches include the use of fiber based laser systems, novel materials for high efficiency pumping and extraction of laser energy, diode pumping and amplification media that include bulk materials shaped as rods or slabs.

Since the required laser technology depends highly on the accelerator requirements, it is clear that not a single technological solution will be appropriate for all applications. Whereas some light source and medical applications need ultra-short laser pulses with pulse duratiosn on the order of a few femtoseconds, others (e.g., colliders) need longer laser pulses. A preliminary design for a laser-plasma-accelerator based collider suggests that laser pulse durations of order 150 fs may be suitable, which opens up material choices that have smaller optical bandwidths but can be directly diode pumped and have excellent thermal properties. These tradeoffs will be the subject of a subsequent workshop.

Acknowledgements

Chapter 1 was written principally by task force panelists Ralph Assmann (CERN), Weiren Chou (Fermilab), Eric Esarey (LBNL), Dino Jaroszynski (U. of Strathclyde), Yun Liu (ORNL), Tor Raubenheimer (SLAC), Mike Seidel (PSI), Toshiki Tajima (LMU MPQ) and Kaoru Yokoya (KEK)

Carl Schroeder and Wim Leemans (LBNL) contributed to the writing of Section 1.1. Valery Telnov (BINP), Chris Barty (LLNL) and Wolfgang Sandner (MBI) made important comments in Section 1.3. Enrico Brunetti (U. of Strathclyde) contributed to Section 2.2.

Chapter 3 was principally written and edited by Wim Leemans (LBNL) with contributions from Bill White (SLAC), Thomas Kuehl (GSI), Frank Stephan (DESY), Siegfried Schreiber (DESY), Franz Tavella (DESY) and Erion Gjonaj (TU Darmstadt).

Chapter 4 was principally written and edited by the section chair, Mitsuru Uesaka (U. of Tokyo) and Ingo Hoffman (GSI). The working group for the section included Kiminori Kondo (JAEA), Manuel Hegelich (LANL), Xueqing Yan (Beijing U.). The chapter was reviewed by Paul Bolton (JAEA), Victor Malka (LOA) and other researchers working on this subject at various places across the world.

Chapter 5 was principally written by Chris Barty (LLNL), Wolfgang Sandner (MBI), Almantas Galvanauskas (U Michigan), Jay Dawson (LLNL), Andreas Tuennermann (Fraunhofer Institute of Physics).

WL gratefully acknowledges the help of Joe Chew with the technical editing.